INVITED REVIEW

https://doi.org/10.1590/2317-4889202120210014

BJGEO Brazilian Journal of Geology

Sequence stratigraphy of clastic and carbonate successions: applications for exploration and production of natural resources

Antonio Jorge Campos Magalhães[1,2,3]*, Daniel Galvão Carnier Fragoso[4,5], Guilherme Pederneiras Raja Gabaglia[4], Gerson Jose Salamoni Terra[6], Anderson Henrique de Melo[4], Peryclys Raynyere de Oliveira Andrade[4], Felipe Guadagnin[7], Francisco Pinheiro Lima-Filho[2]

Abstract

Sequence stratigraphy is a method that unravels the evolution of sedimentation through time and space within sedimentary basins. Nowadays, the exploration and production of natural resources generated by or related to sedimentary processes depend on constructing a chronostratigraphic framework to identify sequences of distinct hierarchies. In clastic and carbonate successions, exploratory studies focus on higher-rank sequences to evaluate the potential of natural resources and to make discoveries. Conversely, lower-rank (i.e. high-frequency) sequences characterize and highlight the spatial and temporal occurrence of natural resource deposits and heterogeneities, necessary for optimizing production. For instance, high-resolution sequence stratigraphic surfaces may indicate the location of placer deposits or coal seams. In the petroleum industry, high-resolution sequence stratigraphy is applied in reservoir zonation and characterization, which are the stratigraphic essence of 3D geological and fluid flow models. Thus, this methodology can guide reservoir management, forecast and optimize production, and increase the ultimate recovery factor. Recent technological innovations such as virtual outcrop models and Ground Penetration Radar have promoted a significant advance in the visualization of surfaces and stacking patterns, making stratigraphic analysis more accurate and efficient than the traditional use of analogs.

KEYWORDS: sequence stratigraphy; natural resource exploration; natural resource production; clastic succession; carbonate succession.

INTRODUCTION

Three major paradigm shifts in sedimentary geology were established in the 20th century (Miall 1995, Catuneanu 2006):

- the concept of flow regimes and the understanding of depositional facies as the outcomes of sedimentary processes operating in depositional environments (Gilbert and Murphy 1914, McKee and Weir 1953, Simons *et al.* 1961, Middleton 1965).
- the incorporation of plate tectonics and geodynamic concepts into the global analysis of sedimentary processes (Bird and Dewey 1970, Dewey and Bird 1970, Dickinson 1971).
- the establishment of sequence stratigraphy (SS) as a stratigraphic analysis method based upon the recognition of depositional trends to unravel the evolution of sedimentation through time and space within sedimentary basins (Payton 1977, Wilgus *et al.* 1988).

As SS embodies the previous paradigm shifts, it applies to any geotectonic setting, sedimentary basin, and type of sediment (i.e. clastic, carbonate, evaporite) at several scales of observation (Catuneanu 2019, Magalhães *et al.* 2020). The process-based sequence stratigraphy method, integrating process-forming deposits and breaks on sedimentation, motivates practitioners to use high-frequency chronostratigraphic correlation and paleogeographic reconstruction to decipher the evolutionary history of a given sedimentary succession with increasing attention to the step-by-step balance between generation and preservation mechanisms (Fragoso *et al.* 2021). It means a change from the lithostratigraphic to chronostratigraphic approach, which is crucial to the economic outcome of any project related to the exploration and production of natural resources (Magalhães *et al.* 2020).

The development of seismic technology enabled the advance and application of SS in the petroleum industry (Payton 1977). Through time, SS application evolved from a

[1]Instituto Dom Luiz, Faculdade de Ciências, Universidade de Lisboa – Lisboa, Portugal. E-mails: jmagalbr@gmail.com, pinheiro@geologia.ufrn.br

[2]Programa de Pós-Graduação em Geodinâmica e Geofísica, Universidade Federal do Rio Grande do Norte – Natal (RN), Brazil.

[3]China-Brazil Joint Geoscience Research Center – Beijing, China.

[4]Petrobras Exploration and Production – Rio de Janeiro (RJ), Brazil. E-mails: galgeo@gmail.com, guilhermegabaglia@hotmail.com, andersonhm@petrobras.com.br, peryclysandrade@petrobras.com.br

[5]Instituto de Geociências, Universidade Federal do Rio Grande do Sul – Porto Alegre (RS), Brazil.

[6]Terra Carbonates – Porto Alegre (RS), Brazil. E-mail: gersonjsterra@gmail.com

[7]Universidade Federal do Pampa – Caçapava do Sul (RS), Brazil. E-mail: felipe@unipampa.edu.br

*Corresponding author.

low-resolution exploratory scale to a high-resolution outcrop and core scale, which is known as high-resolution sequence stratigraphy (HRSS) (Van Wagoner *et al.* 1990, Aitken and Howell 1996). Currently, the method on both scales is part of the routine related to petroleum and other natural resources studies (e.g. placer deposits, coal seams, phosphorites, and water). The effectiveness of such applications depends on how detailed the chronostratigraphic framework of the studied succession is. Case studies that reflect their positive economic impact are rare and usually focused on the oil industry (Catuneanu and Biddulph 2001, Magalhães *et al.* 2020, Melo *et al.* 2020). In carbonate successions, this paper fills a gap related to the control exerted by impermeable layers, which can be mapped through HRSS, on the development of permo-porosity in adjacent carbonate units.

Therefore, this paper aims to:

- present a synthesis of the concepts that support the application of SS on exploration and production of natural resources.
- discuss the development of stratal stacking patterns in variable scales with emphasis on the sedimentary processes that produce sequence stratigraphic surfaces and related natural resource deposits.
- show examples of chronostratigraphic correlations supported by core, log, and seismic data that exemplify the lateral contact among continental to marine deposits.
- discuss the stratigraphic control of impermeable layers on permo-porosity development and hydrothermal mineralization in adjacent carbonate units.
- present the advantages of using geotechnologies on the high-resolution stratigraphic analysis of outcrops.

STACKING PATTERN: A SOLID FOUNDATION FOR STRATIGRAPHIC ANALYSIS

the identification of stacking patterns in a sedimentary succession is the core of sequence stratigraphic analysis. Stacking patterns correspond to the depositional style produced within a sedimentary system in response to the interplay between sedimentation and base-level fluctuations through time. In general, they are interpreted as the record of depositional systems displacement landward or basinward, linked or not to the shoreline trajectory (e.g. Catuneanu *et al.* 2011).

There are four stacking patterns in the sedimentary record: progradation, retrogradation, aggradation, and degradation (Fig. 1; Van Wagoner *et al.* 1990, Neal and Abreu 2009). They may be identified at different scales, for instance, by grain size upward trend in clastic shallow-marine deposits (Posamentier and Allen 1999), vertical stacking of architectural elements or facies associations (Magalhães *et al.* 2016, 2020), well logs accurately calibrated with rock data (Van Wagoner *et al.* 1990), and reflector termination patterns at seismic scale (Grabau 1906, Mitchum 1977, Mitchum and Vail 1977).

The recognition of stacking patterns is closely related to and may vary with the hierarchical rank of the studied interval (e.g. Fragoso *et al.* 2021). Hence, it is fundamental to identify the criteria that marks the change in the observed stacking

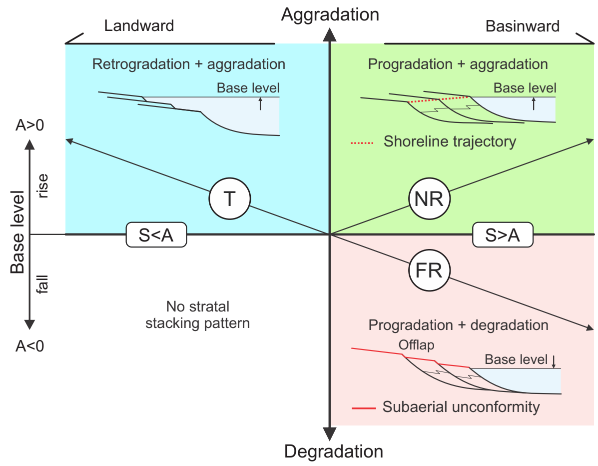

T: transgression; NR: normal regression; FR: forced regression; A: accommodation; S: sedimentation.

Figure 1. Stacking patterns and relative depositional systems trajectories in downstream settings (modified from Catuneanu 2017). The stratal geometry applies to a seismic scale. Conversely, the stacking of architectural elements relates to a high-resolution scale.

patterns before mapping their related stratigraphic surfaces (e.g. Magalhães *et al.* 2020). For instance, offlap is a typical stratal termination observed at the top of forced regression clinoforms in low- to medium-resolution seismic volumes. In contrast, coarsening-up cycles within each clinoform typify high-resolution trends recognized in cores, well logs, or outcrops at a high-resolution scale (e.g. Melo *et al.* 2020).

Stacking pattern in clastic successions

A systems tract corresponds to a linkage of contemporaneous depositional systems forming the subdivision of a sequence (Brown and Fisher 1977). In the geological record, a systems tract consists of a relatively conformable succession of genetically related strata, which shows a specific stacking pattern bound at the base and the top by stratigraphic surfaces (Catuneanu *et al.* 2011). An understanding of regression, transgression, and the expected systems tracts in clastic successions through time is offered via comparing accommodation and sedimentation rates (Fig. 2). The interplay of these factors promotes changes in stratal stacking patterns that define key sequence stratigraphic surfaces (for a thorough review of sequence stratigraphic surfaces, see Catuneanu 2006).

The sedimentation rate in a clastic succession can be defined as the rate of terrigenous sedimentary supply. In other words, the mass of the source area transformed into particles through erosion processes and drained downstream to the transfer and basin areas (Fig. 3). The transfer compartment is characterized by the dynamics of gravitational flows, rivers, wind, and glaciers that transport sediments from the erosion to the sedimentation compartment. In a clastic succession, the study of these dynamics is essential in the understanding of the stratigraphic record (e.g. Romans *et al.* 2016).

In the downstream region, the interplay of eustasy, subsidence, and sediment supply controls the sedimentary dynamics (e.g. Jervey 1988). In these areas, the standard nomenclature of the systems tracts is traditionally used (Fig. 2).

In contrast, in the upstream area, the combined action of tectonics and climate variations result in fluctuations in energy and sediment flow that characterize the low- and high-accommodation system tracts. For example, in fluvial settings, the former comprises high-energy, sand-rich amalgamated-channels, whereas the latter consists of fine-grained, low-energy overbank facies (Wright and Marriott 1993, Shanley and McCabe 1994).

The basin is the depositional site that stores the sediments drained along the transfer area (Fig. 3). In this part, various continental to marine clastic depositional environments are developed and subjected to variations in sediment flow energy and changes in base level, which modify accommodation and sedimentation (Castelltort and Van Den Driessche 2003). Even though the balance of the sedimentary system is always affected by autogenic factors, the cyclical record of

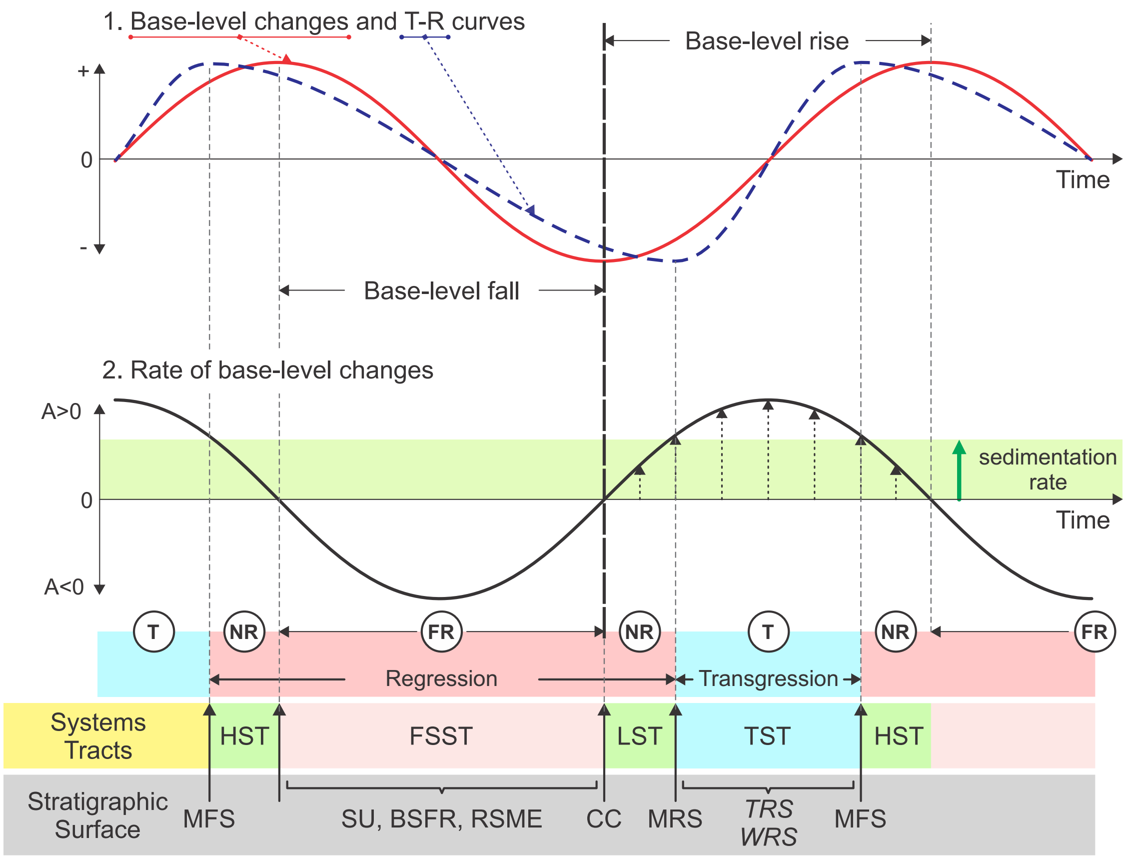

T-R: transgressive-regressive; HST: highstand systems tract; FSST: falling stage systems tract; LST: lowstand systems tract; TST: transgressive systems tract; MFS: maximum flooding surface; SU: subaerial unconformity; BSFR: basal surface of forced regression; RSME: regressive surface of marine erosion; CC: correlative conformity; MRS: maximum regressive surface; TRS: tidal-ravinement surface; WRS: wave-ravinement surface.

Figure 2. The development of stratal stacking patterns during regression and transgression results from the interplay between accommodation and sedimentation (modified from Catuneanu 2006, Fragoso *et al.* 2021). The base-level curve varies from a minimum to a maximum, and so does the rate of the base-level change (i.e. accommodation). To clarify, both are presented as symmetrical sine curves and the sedimentation rate is constant even though they are much more complex and asymmetric in nature.

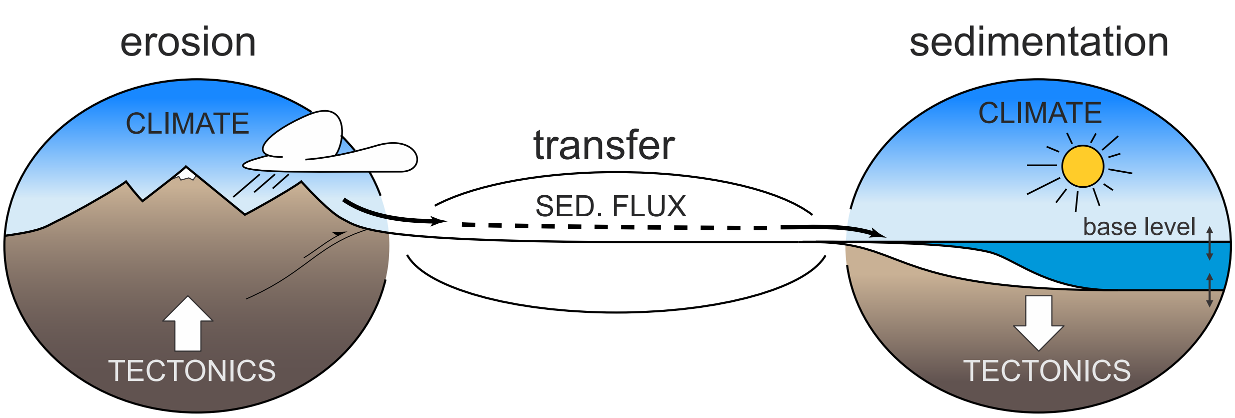

Figure 3. Schematic illustration of the three main compartments that make up sedimentary systems. Each compartment is characterized by a dominant process: erosion, transfer and sedimentation (Castelltort and Van Den Driessche 2003).

these variations through time is primarily controlled by allogenic factors (Holbrook and Miall 2020). The allogenic factors are related to eustasy, climate, and tectonic mechanisms that control the generation-preservation sedimentary dynamics (Fragoso *et al.* 2021). The effect of these mechanisms in the depositional systems results in regression (displacement basinward) or transgression (displacement landward), which is recognized from the stacking pattern in the stratigraphic record. Regression happens when more proximal depositional systems or their components overly more distal ones. Conversely, transgression occurs when more distal depositional systems or their components overly more proximal ones. The displacements controlled by allogenic factors affect large areas of a sedimentary basin, supporting stacking pattern stratigraphic correlations (Fragoso *et al.* 2021).

Stacking pattern in carbonate successions

The principles and concepts of SS were developed through the study of clastic successions. The application in carbonates is not straightforward due to an intrinsic characteristic: sedimentary carbonate constituents are *produced within* the depositional locus, whereas clastic sediments *must be transported* from the source area to the basin (Fig. 3). Carbonate sedimentation depends on carbonate factories switching and production rates, which may work in an opposite way to the sediment supply versus accommodation relationship observed in clastic systems (Pomar and Haq 2016). According to Pomar (2020), carbonate production depends on five "W's": When produced; What produced; Where produced, hoW produced, and Where accumulated. The 5W's summarize the carbonate's dependency on the evolution through time of organisms that form the rock, the environmental and hydrodynamic conditions, the type of accommodation (i.e. physical or ecological), and the type of substrate on which the sediment is deposited or produced (Fig. 4). The lag time between carbonate grain production and deposition is a key factor that explains the higher productivity of shallow-marine carbonate factories during the highstand systems tract (HST) in comparison to the transgressive systems tract (TST) (Handford and Loucks 1993, Jones 2010). Besides, differently from clastic grains that remain unconsolidated for a long time in the depositional setting, carbonate sediments are heavily affected by the diagenetic processes of cementation and dissolution soon after deposition and hence no longer available for reworking (G. Terra unpublished data).

In a lacustrine setting, the interplay of lake level and sediment supply alternates carbonate and clastic deposition in a dynamic much different from the observed in marine environments (Bohacs *et al.* 2000, Renaut and Gierlowski-Kordesch 2010). For instance, in a balanced-fill lake type, a lag time is required for the lake bottom to turn into a semi-consolidated substrate and switch on the carbonate factory. Moreover, in this lake-type, the efficiency of the carbonate factory is the at it's highest during HST and falling stage systems tract (FSST) and insignificant throughout the TST (Magalhães *et al.* 2020).

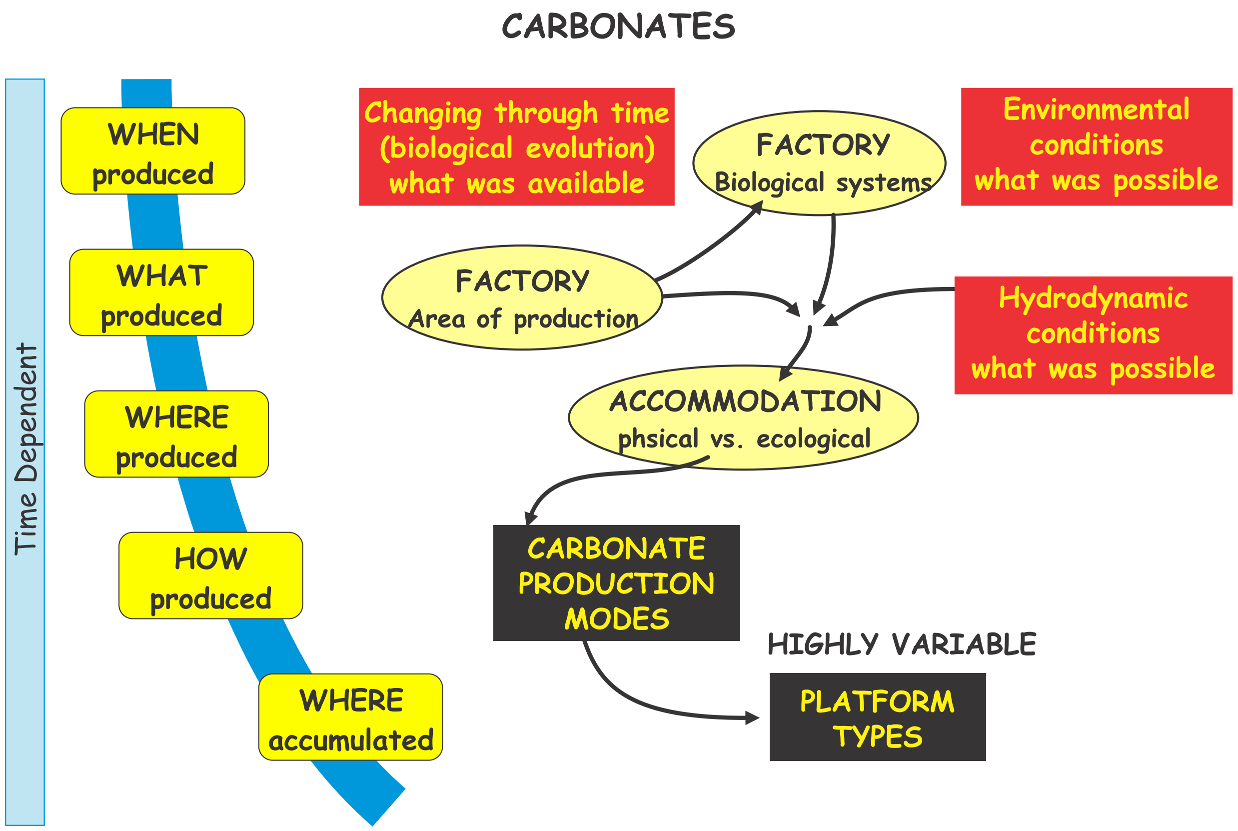

Source: modified from Pomar (2020).

Figure 4. Key factors on carbonate sedimentation. Understanding carbonate systems require answering the five "W": When, What, HoW, Where was produced, and Where was accumulated.

The bulk of carbonate sediments are deposited very closely to the location where they are produced, and thus the higher the production, the higher the accumulation of sediments (Handford and Loucks 1993). As a general rule, accumulation is directly dependent on productivity, except for tidal flats (where production is low, but accumulation is high) and carbonate slopes (where accumulation from gravitational processes outpaces local production) (Handford and Loucks 1993). The interplay between sediment production and accommodation defines the stacking pattern of shallow-marine carbonates (Fig. 5).

Since the shallow-marine carbonate has a strong organic influence, the carbonate factory reaches its maximum efficiency in the photic zone (Fig. 6). Hence, the substrate morphology exerts great control over the carbonate sequence development. The comparison between clastic and shallow-marine rimmed carbonate shelves indicates opposite behavior in terms of accumulation in lowstand and highstand systems tracts. The optimum behavior for clastic shelves is lowstand, whereas the optimum behavior for carbonates is the highstand (Fig. 7). Table 1 presents the main aspects that control clastic and carbonate deposition.

It is noteworthy that the classical stratal geometry applied to clastic successions is not straightforward when it comes to carbonates. The detailed analysis of the skeletal composition of carbonate facies and the resulting stacking pattern is the criteria that identifies sequence stratigraphic surfaces in

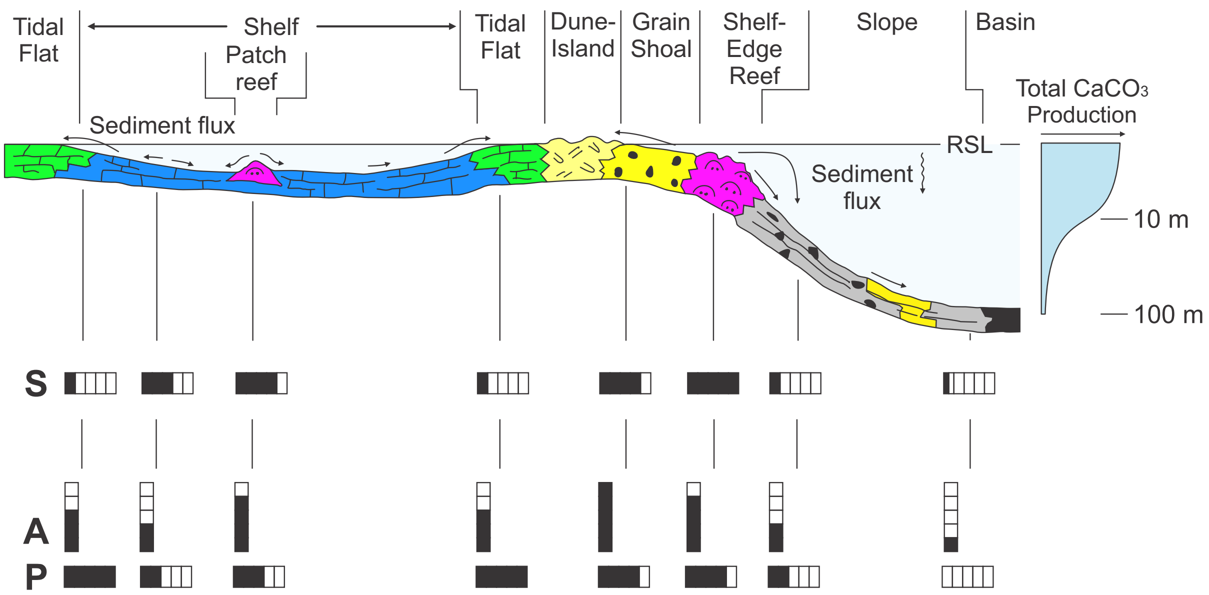

S: production rate; A: aggradation; P: progradation. Source: modified from Handford and Loucks (1993).

Figure 5. Carbonate sediment productivity and accumulation determines the aggradational or progradational stacking pattern and varies with depth and depositional setting. The black rectangles represent the production and the aggradational or progradational rate in the marine environment.

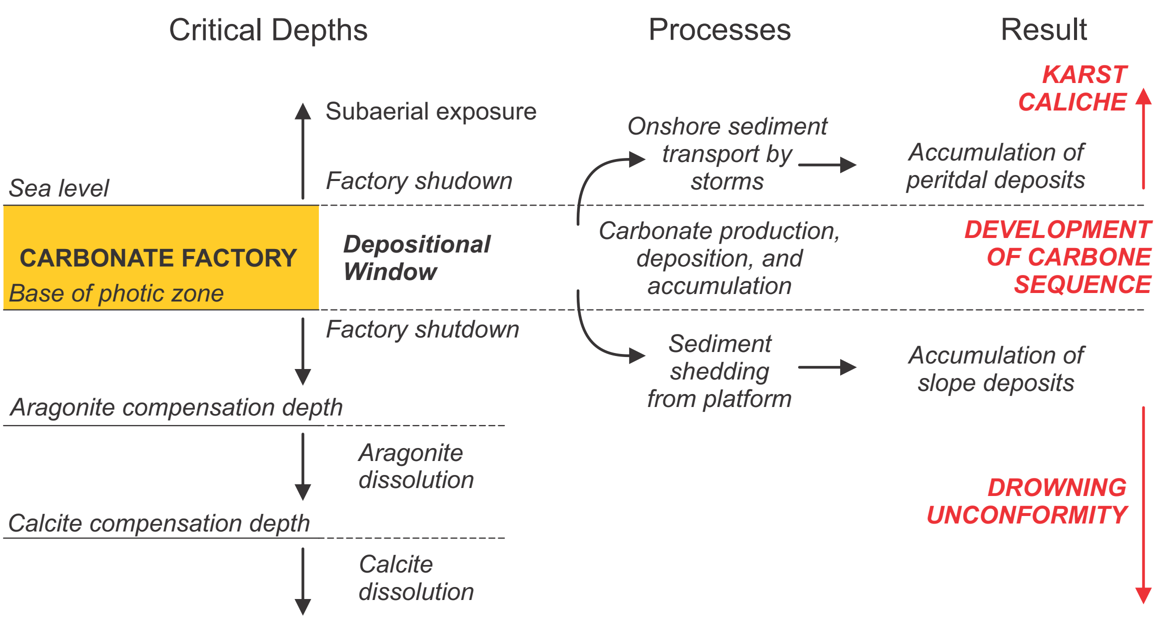

Source: Jones (2010).

Figure 6. Critical depths and processes that control the development of carbonate sequences.

carbonate successions (Pomar and Haq 2016). The spectacular outcrop in Cape Blanc, Mallorca, Spain, is an example of identifying carbonate stacking patterns (Pomar 1993, Pomar and Haq 2016). The interpretation of systems tracts highlights sedimentation evolution through time, based on the vertical stacking and lateral facies contact of this Miocene rimmed shallow-marine platform (Fig. 8). The TST is generally unidentifiable since there is no landward migration of depositional facies. During the HST, the system keeps up an enhanced sediment production that allows for basinward export. The HST is progradational and capped by a subaerial unconformity. The FSST consists solely of reefal facies that prograded over the HST fore-reef while coeval erosion took place on the emerged reef and lagoon. The Maastrichtian-Paleocene Balbuena Sequence in Salta Basin, Argentina is a world-class example of a stacking pattern and cyclicity in a lacustrine carbonate in which

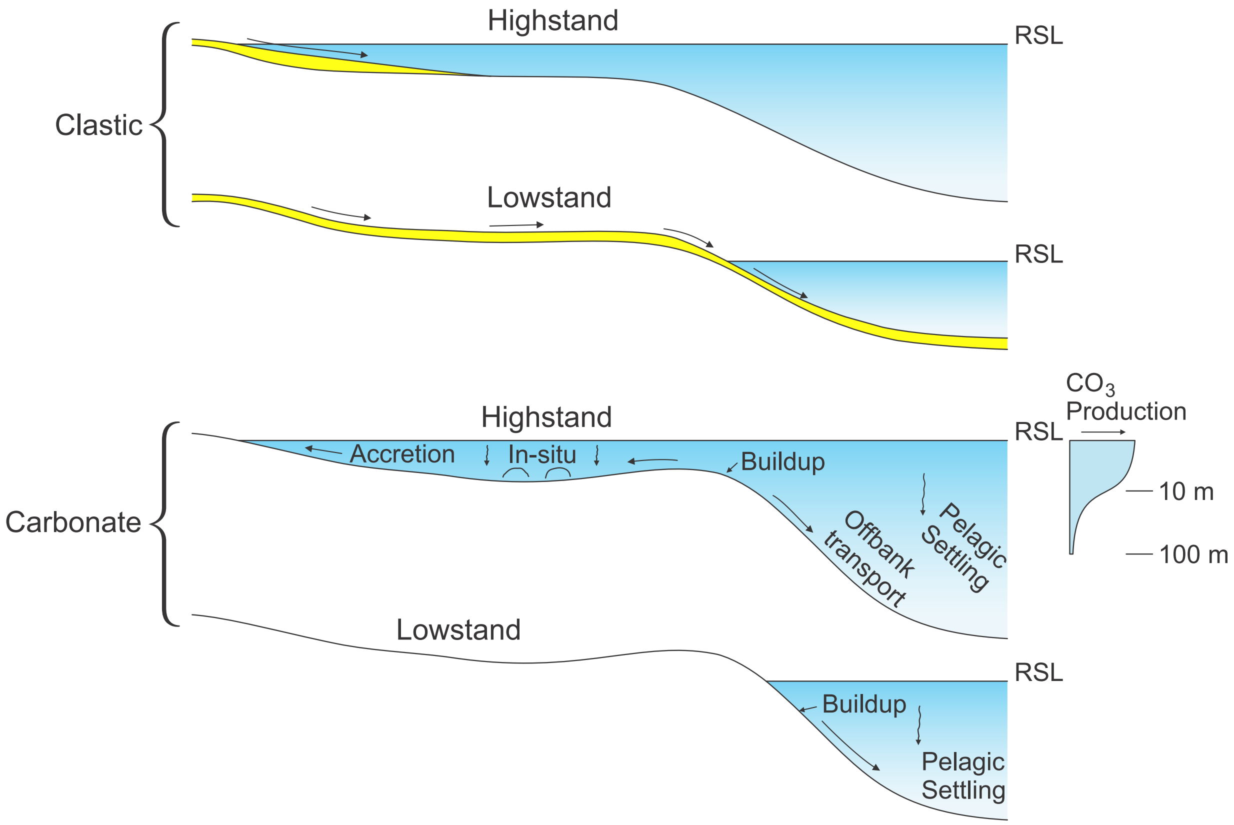

Source: modified from Handford and Loucks (1991).

Figure 7. Carbonate vs. clastic sedimentation.

Table 1. Differences between clastic and carbonate sediments.

Clastic	Carbonate
Formed via simple processes of erosion, transfer and sedimentation	Formed by complex processes: When produced; What produced; Where produced, HoW produced and Where accumulated
Unconstrained by time	Time-dependent due to organic influence, reflecting the evolution of life on Earth
There is no relationship between the location the sediment was formed, and the volume deposited	The majority of sediments are deposited closely to the location where they were produced
As siliciclastic constituents are always available, environmental changes have an immediate effect on sedimentation	The carbonate fabric requires time to produce constituents (lag time), and environmental changes do not have an immediate effect on sedimentation
Sediments remain unconsolidated in the depositional environment and available for reworking	Sediments are heavily affected by diagenesis (cementation and dissolution) soon after deposition and no longer available for reworking
There is no relationship between water depth and the amount of sediment available for deposition	The bulk of production occurs in shallow water (photic zone) due to organic influence
Substrate morphology exerts little control on the type of deposits	Substrate morphology exerts a great control on the type of deposits
Does not produce organic build-ups	Produces rigid organic build-ups or reefs that affect the environment hydrodynamics and can follow relative sea-level changes (i.e. keep up, catch up)
Base level equals wave base level in marine and lake environments	Base level equals the sea or lake level

high-frequency Transgressive-Regressive (T-R) cycles were controlled by the ratio between precipitation (P) and evaporation (E) rates. A high P/E ratio implies a wet climate, the rise of phreatic and lake levels, as well as an increase in terrigenous influx. A Low P/E ratio means a dry climate, the fall of phreatic and lake levels, substantial reduction of terrigenous influx and carbonate sedimentation. The resulting succession records cyclic fine-grained siliciclastic and carbonate strata (Bento Freire 2012, Pedrinha 2014, Roemers-Oliveira *et al.* 2015, Bunevich *et al.* 2017, Magalhães *et al.* 2020).

Systems tracts: the relative displacement of depositional systems

Forced regression

Forced regression happens throughout the base level falling stage (Fig. 2). It means that the depositional systems ought to migrate abruptly towards the depocenter following the base-level fall and coeval subaerial exposure landwards. For example, the relative sea-level fell approximately 130 m and exposed a vast area in the Thailand Gulf during the last glacial age (Posamentier 2001, Lear *et al.* 2020). Subsequent transgression flooded this region and the maximum water depth of around 90 m is currently recorded. (Reijenstein *et al.* 2011).

The base-level fall is not instantaneous. During this stage, the progradation progresses step-by-step basinward, concomitant with the development of subaerial exposure on land (Catuneanu 2006). The youngest terrace is located in the lowest topography compared to its predecessors (Fig. 9). At a seismic scale, this pattern is recognized through offlap stratal termination in which the bottom surface of the oldest clinoform marks the basal surface of forced regression (Mitchum 1977, Hunt and Tucker 1992).

At the onset of the forced regression, the paleo-seafloor surface represents the basal surface of forced regression (BSFR; Hunt and Tucker 1992). The base-level fall may trigger wave scouring in locations where the wave equilibrium profile is lower than the paleo-depositional surface (Bruun 1962, Plint 1988, Dominguez and Wanless 1991). Wave scouring during forced regression forms the regressive surface of marine erosion (RSME; Plint 1988). The forced regression ends when the base level reaches its minimum (Fig. 2). At this moment, the top of the youngest clinoform associated with offlap marks the correlative conformity (CC). This surface approaches the paleo-seafloor and connects to the subaerial unconformity (SU) at the paleo-shoreline (Hunt and Tucker 1992). Therefore, the stacking pattern of forced regression combines degradation and progradation (offlap) at a low-resolution (Fig. 9). In the high-resolution, the forced regressive stacking pattern is revealed by hummocky cross-strata filling gutter casts that characterize the sharp-based forced regressive shoreface facies overlying the RSME (Fig. 9B), or by gradationally based forced regressive deposit overlying the BSFR (Catuneanu 2006, Magalhães *et al.* 2021). In the parts where it's missing, the FSST is represented by the SU (Magalhães *et al.* 2020).

During forced regression in marine environments, accommodation is only available seaward where deposits in this stage are preserved. High-density turbidites may turn into significant reservoirs, such as the Upper Eocene strata of Albacora Field in the Campos Basin, Brazil (De Gasperi and Catuneanu 2014). Besides, SU development under suitable climatic conditions may favor the development of mature paleosol and bauxite deposits (Zhukov and Bogatyrev 2012). Long-term subaerial exposure is also highly conducive to intense erosive and reworking processes that may cause the transportation of heavy minerals through fluvial systems. If these sediments eventually reach the shoreline, they may be concentrated by

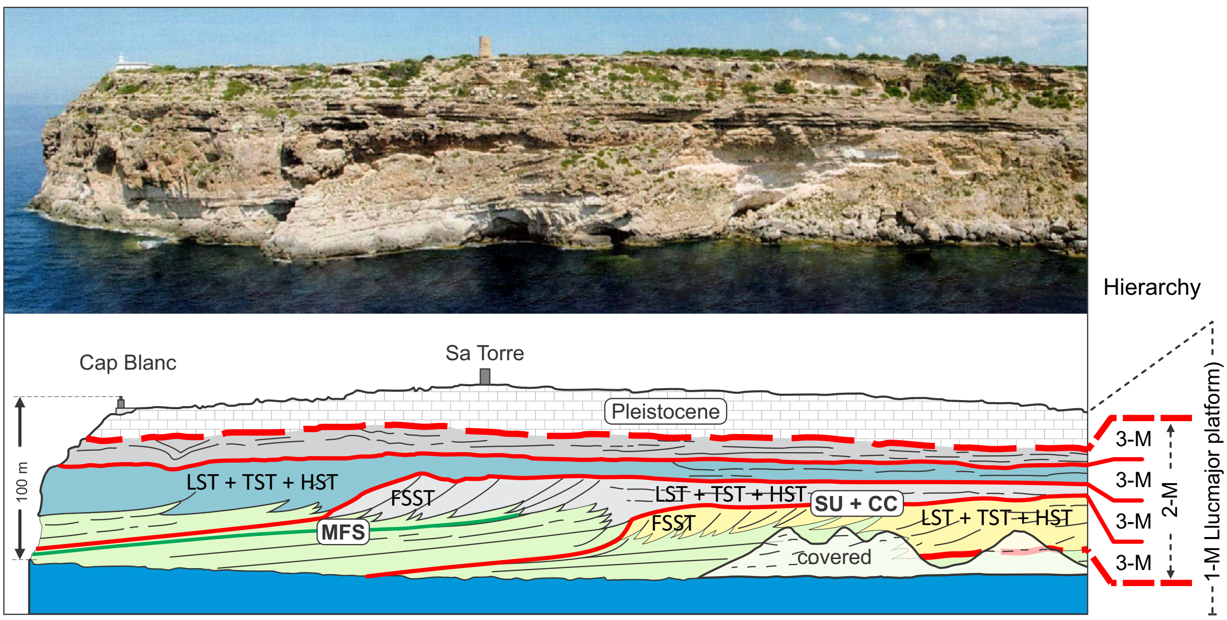

Figure 8. Facies architecture and sequence stratigraphy interpretation of a rimmed carbonate platform in Cap Blanc, Mallorca. The Llucmajor Platform consists of a stratigraphic unit subdivided into four hierarchic units (1-M, 2-M, 3-M, and 4-M) bound by SU and related CC basinward (modified from Pomar 1993, Pomar and Haq 2016). SU is related to karstic features in each hierarchy. The photo exhibits the youngest outcropping 2-M unit and its youngest three 3-M units. Internal subdivision of 3-M units, shown by progradation of reef complexes, stands for 4-M units and is not visible in this picture.

wave action and form placer deposits associated with beaches or overlying high-frequency RSME (Catuneanu, 2006).

Normal regression

During the early and late stages of base-level rise, the sedimentation rates outpace the positive but very low accommodation rate and sedimentation immediately fills any available space (Fig. 2). It means that the sediment excess has no option other than to aggrade and move basinward, thus triggering normal regression (Catuneanu, 2006). Therefore, the stacking pattern of normal regression combines aggradation and progradation (Fig. 10).

The increase in accommodation throughout the early stage of base-level rise may favor aggradation at the expense of progradation (i.e. thicker aggradational strata and less prominent progradational deposits). Conversely, the decrease in accommodation throughout the late stage of base-level rise may promote progradation with little aggradation (Catuneanu *et al.* 2011). It is noteworthy that as accommodation is always positive, subaerial exposure is not likely during normal regression. The presence of subaerial exposure features during normal regressive trend indicates higher-frequency base-level fall, and therefore, higher-frequency breaks in such trend (e.g. Magalhães *et al.* 2021). Moreover, normal regression does not happen instantaneously. Instead, it is usually punctuated by higher-frequency transgressions that promote breaks in the overall regressive trend. Such breaks are recognized in the rock record as muddy strata interlayered and separating prograding clinoforms (i.e. allomembers) as seen in regional cross-sections (e.g. Bhattacharya and Walker 1991, Bhattacharya 1993).

The positive accommodation during lowstand systems tract (LST) traps sedimentation on the shallow-marine to fluvial settings, and only low-density flows feed turbidites basinwards (Catuneanu 2006). Deposits such as the Cretaceous fluvial sandstones of the Potiguar Basin (Melo *et al.* 2020) and the Oligocene-Miocene turbidites in Marlim Field, Campos Basin (Bruhn *et al.* 2003) are potential hydrocarbon reservoirs. In the beginning of the LST, low accommodation rates enable preserving high-energy fluvial and placer deposits overlying the SU. Good examples of this kind of occurrence are the Lavras conglomerate Mesoproterozoic in the Chapada Diamantina in Brazil (Magalhães *et al.* 2016), and the gold rich Zandpan conglomerate, Late Archaean Witwatersrand Basin, in South Africa (Catuneanu and Biddulph 2001). During HST, progradation of shoreface and delta systems provide suitable hydrocarbon reservoirs, as observed in the Eocene of Niger Delta, Nigeria (Tuttle *et al.* 1999) and the Lower Cretaceous of the Recôncavo Basin (Della Fávera *et al.* 2019).

The Maximum Regressive Surface (MRS; Helland-Hansen and Martinsen 1996) marks the end of the lowstand normal regression. Thererfore, MRS is a surface close to the fluvial topset and the paleo-seafloor at the top of the youngest clinoform associated with the lowstand normal regression. Therefore, MRS marks the onset of the transgression.

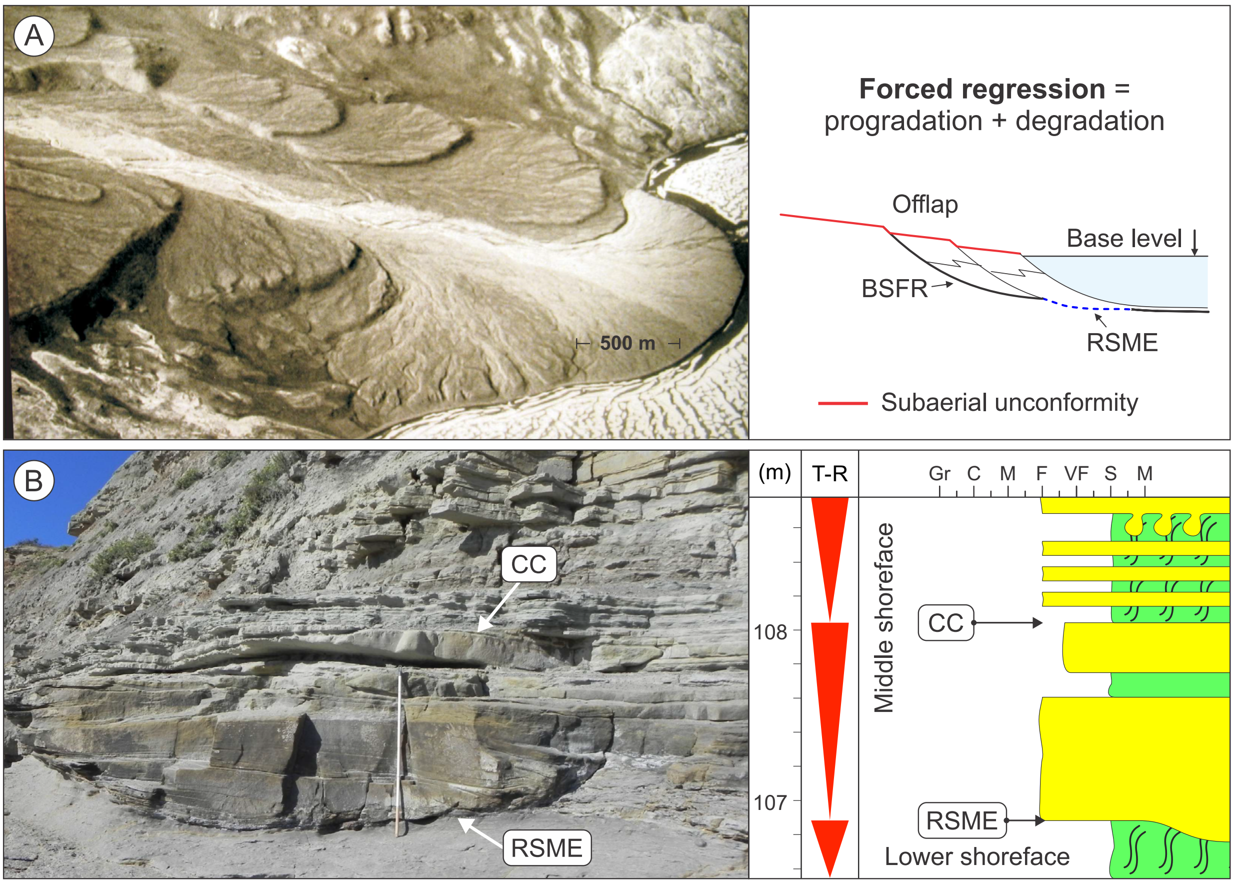

Figure 9. Forced regressive stacking pattern expression in (A) low-resolution modern analog landscape, Canadian shield (Catuneanu 2006) and the equivalent progradation and degradation patterns seen in seismic lines. (B) Forced regressive sharp-based hummocky cross-bedded sandstone filling gutter casts is bound by RSME and CC (Bathonian-Early Callovian, Lusitanian Basin; modified from Magalhães *et al.* 2021). Stick is 1.2 m long.

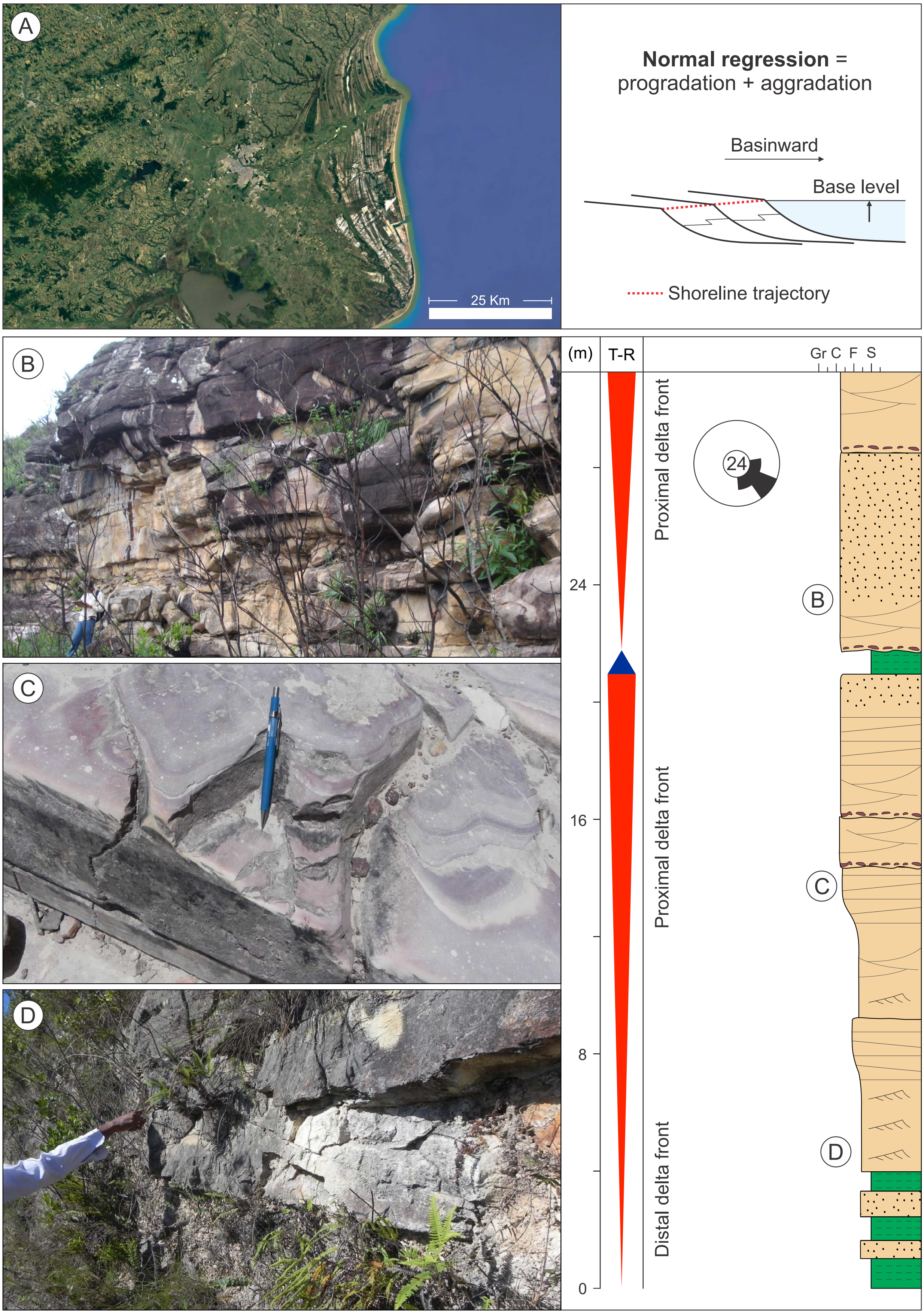

Figure 10. Normal regressive stacking pattern expression in (A) low-resolution modern analog landscape, wave dominated Paraíba do Sul delta in Southern Brazil (Google Earth), as well as the equivalent aggradational and progradational patterns seen in seismic lines. A high-resolution normal regressive deltaic succession exhibits thickening- and coarsening-upward patterns (B, C and D) that fine-grained delta plain deposits may cap. Example from the fluvial dominated Mesoproterozoic Açurua Formation in the Chapada Diamantina Basin, Brazil (modified from Magalhães *et al.* 2015). Paleocurrent directions are indicated.

Transgression

Transgression occurs when the accommodation rate outpaces the sedimentation rate. It results from excess space compared to the available sediment(Fig. 2; Catuneanu 2006). Therefore, following the MRS, all depositional systems or their components start moving landwards. Most of the sedimentary load is trapped within the aggrading fluvial and transitional systems, which are eventually overlain by marine deposits (Loutit *et al.* 1988, Galloway 1989). However, transgressions do not happen instantaneously. Instead, it is more likely to be punctuated by higher-frequency regressions that promote breaks in the transgressive trend. Such breaks are recognized in the rock record of shallow marine or estuarine systems by erosive truncating surfaces (SU) at the base of sand-rich bars or tidal channels (Fig. 11; e.g. Magalhães *et al.* 2016).

During transgression, waves and tides may scour the substrate. Wave scouring during transgression produce wave-ravinement surface (WRS) in the upper shoreface, at locations where the wave equilibrium profile is lower than the paleo-depositional surface (Bruun 1962, Swift 1975, Plint 1988, Dominguez and Wanless 1991). Wave scouring may concentrate lag or placer deposits, as demonstrated in the Ordovician of Sardinia, Italy, and the Armorican Massif in Western France (Pistis *et al.* 2016). The tidal-ravinement surface (TRS) is a scour cut by tidal currents in coastal environments during transgression (Allen and Posamentier 1993). This surface is likely preserved "in a transgressive river-mouth setting, where the rates of aggradation of the estuary-mouth complex outpace the rate of subsequent wave-ravinement erosion" (Catuneanu 2006, p. 153).

The transgressive stacking pattern comprises a combination of aggradation and retrogradation (Fig. 11). Therefore, the marine sedimentation progressively retrogrades, pushing marine, estuarine, coastal, and fluvial settings landwards forming onlap stratal terminations, as seen in the seismic lines (Galloway 1989, Catuneanu 2006). Transgressive systems tracts comprise important hydrocarbon reservoirs. These include the Cretaceous fluvial and estuarine deposits in the Potiguar Basin, Brasil (Melo *et al.* 2020), and the Early Cretaceous Athabasca Oil Sands, in Western Canada (Mossop 1980). Besides, the upwelling of nutrients during transgression may favor the development of phosphorite deposits in shallow-marine strata (Abram *et al.* 2011, Abram and Holz 2020, Kechiched *et al.* 2020). At the end of the transgression, the Maximum Flooding Surface (MFS) marks the change from transgressive (below) to normal regression (highstand, above) stacking pattern (Frazier 1974, Posamentier *et al.* 1988, Van Wagoner *et al.* 1988, Galloway 1989). The high-water table in coastal to continental areas, coupled with a suitable climatic condition, would favor the formation of coal seams associated with MFS (Bohacs and Suter 1997, Holz *et al.* 2002).

Hierarchy on sequence stratigraphy

The sequence stratigraphy analysis characterizes cyclic units at multiple scales (Catuneanu 2019). From facies cycle to basin scale, stacking patterns and stratigraphic surfaces are recognized as sequence elements (Fragoso *et al.* 2021). It is noteworthy that systems tracts were defined at the seismic scale, even though no scale is indicated in its definition (e.g. Brown and Fisher 1977). With standard sequence stratigraphy methodology and nomenclature, the systems tracts became applicable for any spatial and temporal scales (Catuneanu *et al.* 2011). However, adaptations are necessary, especially in high-resolution sequences (Magalhães *et al.* 2020). This way, a ranking system for sequences and their internal elements is crucial for the sequence stratigraphy workflow.

Hierarchy of stratigraphic surfaces

Depositional facies and surfaces result from sedimentary processes (Fig. 12). A depositional surface is a boundary that envelops discrete rock bodies and can be recognized within individual facies, from lamination to bedding planes, or at concordant non-erosional and discordant erosional contacts between facies or facies associations (e.g. Brookfield 1977, Allen 1983, Miall 1985, Einsele *et al.* 1991). A depositional surface is categorized as a key stratigraphic surface when it marks a change in stratal stacking pattern (Catuneanu 2006, Catuneanu *et al.* 2011).

Both autogenic and allogenic controls may contribute to producing any sedimentary or stratigraphic surface. However, even though autogenic factors may create a stacking pattern, the recurrence of stratigraphic surfaces indicates a regular allogenic mechanism-controlled sedimentation (Fragoso *et al.* 2021). Nevertheless, regardless of their periodicities, the influence of autogenic and allogenic factors on sedimentary processes is tied to the surface generation scale (i.e. the highest stratigraphic frequency). As there are no stratigraphic surfaces formed by sedimentary processes that *only* operate at a low frequency, stratigraphic surfaces of any hierarchy are always anchored to the lowest-rank sequence stratigraphic unit. Therefore, a high-frequency stratigraphic surface may be a *candidate* to a higher order, and the *candidate* surface keeps its intrinsic character regardless of its hierarchical rank. Ranking stratigraphic surfaces is fundamental to determining the boundaries of long-term transgressive or regressive trends that separate systems tracts of the higher-order sequences (Magalhães *et al.* 2020).

The superimposition of similar-nature stratigraphic surfaces is a natural consequence of the long-term permanence of identical sedimentary processes operating in the same location. In this situation, the resolution is likely to be lost, and the surface marks a boundary of long-term transgressive or regressive trend (Magalhães *et al.* 2020). For instance, distinct high-frequency MRS may not be recognized in the aggrading coastal to fluvial settings since they superimpose each other at the location dominated by sediment by-pass. This place may be identified in seismic sections through toplap stratal termination. Several high-frequency MFS amalgamate towards the depocenter. The combined effect of low sedimentation rate during long-term transgression induces the generation of "condensed section" recognized in seismic data (Loutit *et al.* 1988, Galloway 1989). Subaerial unconformities superimpose each other landwards or induce a "cryptic sequence boundary" (sense Miall and Arush 2001) as long as a long-term forced regression persists. Therefore, the hiatuses associated with SU become more extensive landward than basinward.

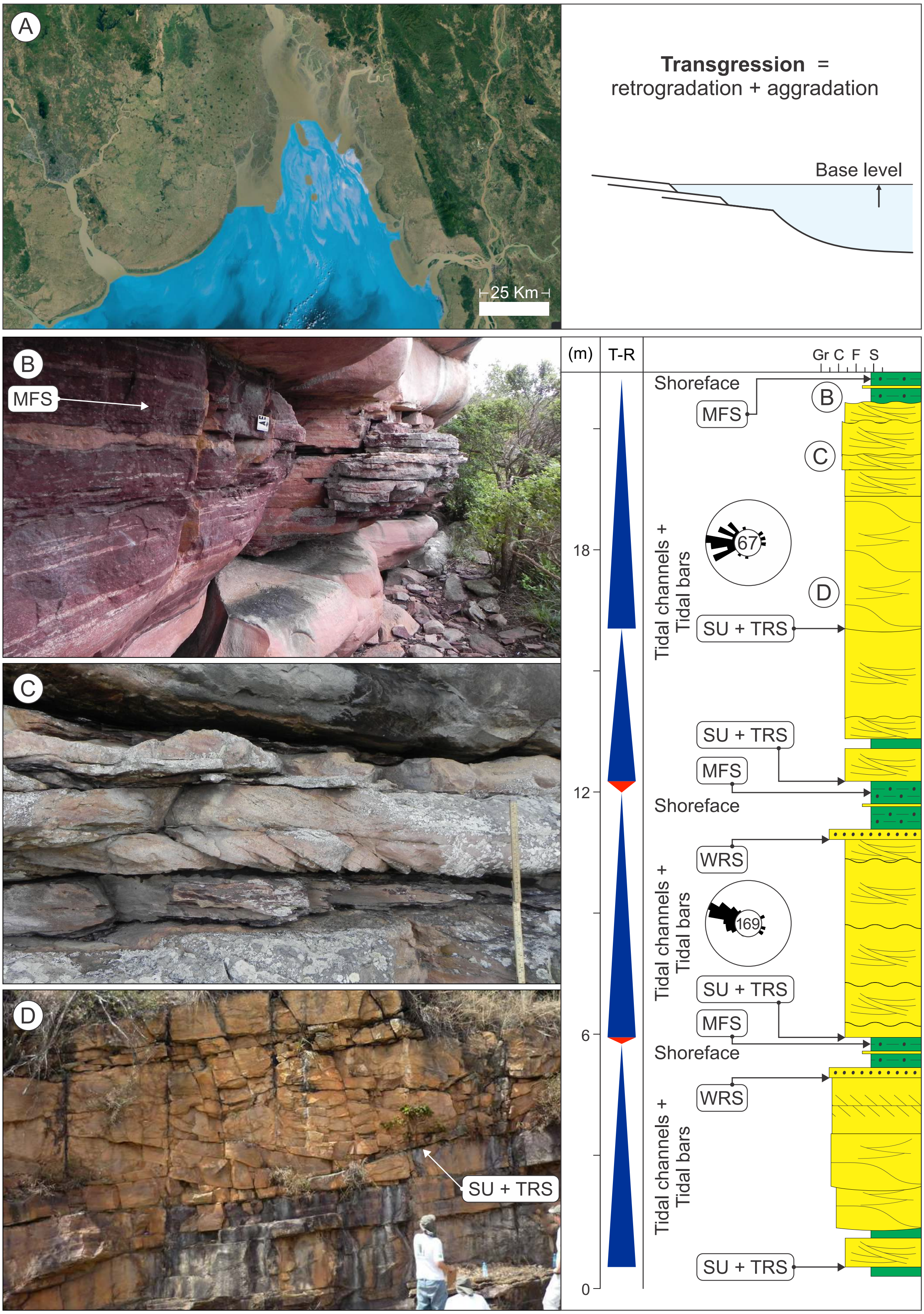

Figure 11. Transgressive stratal stacking pattern expression in (A) low-resolution modern analog from the Sittang River estuary, Myanmar (Google Maps), and the equivalent classic stratal geometry seen in seismic lines. (B, C and D) High-resolution retrogradational stacking pattern exhibited by estuarine sandy tidal channels and bars (in yellow) overlain by fine-grained shoreface strata (in green). The transgressive stacking is punctuated by superimposed subaerial unconformity and tidal-ravinement surfaces (Mesoproterozoic Tombador Formation, Chapada Diamantina Basin, NE Brazil, modified from Magalhães *et al.* 2014). Paleocurrent directions are indicated.

Stratigraphic surfaces of the same nature cannot be superimposed when their sedimentary forming processes operate in different locations during a long-term transgressive or regressive trend. It occurs in wave-ravinement surface (WRS), tidal-ravinement surface (TRS), and the regressive surface of marine erosion (RSME). During long-term transgression, high-frequency WRS is only formed at the specific location where wave equilibrium profile is lower than the depositional surface. This location shifts landwards at the next high-frequency transgression event, during which transgressive strata overlie the previous WRS. Therefore, WRS surfaces cannot be superimposed since they are separated by transgressive strata (Fig. 13). The same happens to TRS if not replaced by WRS. In this situation, the two transgressive ravinement surfaces are separated by estuary-mouth complex deposits (Catuneanu 2006). The same approach is related to high-frequency RSME, which is generated in distinct locations towards the depocenter during long-term forced regression. That is why there is neither medium- to low-frequency WRS diachronically truncating the overall lower-frequency TST nor medium- to low-frequency RSME diachronically truncating the overall lower-frequency FSST. Besides, long-term transgressive and regressive trends are generally punctuated by high-frequency regressions and transgressions, respectively (Fig. 13).

The assignment to different hierarchical levels is only possible for SU, MRS, and MFS. Conversely, WRS, TRS, and RSME are only tied to their highest-frequency sequence hierarchy. The scenarios mentioned above operate at ideal conditions that control the interplay of accommodation and sedimentation rates, generating the four classic systems tracts (i.e. HST, FSST, LST, and TST). Catuneanu (2019) presented unusual scenarios in which SU develops during transgression or SU does not develop during forced regression.

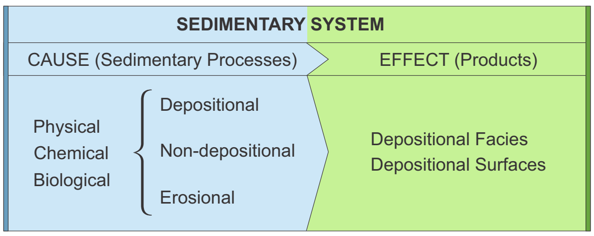

Figure 12. Cause and effect relationship in the sedimentary system (modified from Selley 1970). Sedimentary processes produce depositional facies and surfaces.

Sequence stratigraphy workflow

Sequence stratigraphy may adequately address the research, exploration, and production of any natural resource deposits generated by or related to sedimentary processes. The SS workflow starts with understanding the tectonic setting and regional context of depositional systems (Fig. 14). Depending on the scale of the data available, the method can be constrained to low-resolution (i.e. supported by regional-scale data) or may progress to high-resolution studies (based on outcrop, reservoir-scale data). The application of SS in low-resolution determines long-term depositional trends aiming to evaluate the potential of natural resources and make discoveries (Catuneanu 2006). Conversely, the high-frequency stratigraphic analyses unravel the spatial and temporal distribution of petroleum reservoirs and natural resource deposits (i.e. the external geometry, connectedness, and heterogeneities) to optimize production (Magalhães *et al.* 2020). Therefore, SS application at both scales has a strong positive economic impact in the outcome of exploration and production projects.

Besides, HRSS also helps in identifying recurrent mappable stratigraphic surfaces that control the genesis or distribution of natural resource deposits, such as SU associated with placer deposits or MFS related to coal seams. Such surfaces provide the closest approximation to the timelines on cross-sections or correlations (Catuneanu 2006), further below the resolution of biostratigraphic methods. Mappable sequence stratigraphic surfaces must be correlated throughout the study area before facies representation. The correlation individualizes systems tracts with their specific stacking pattern and

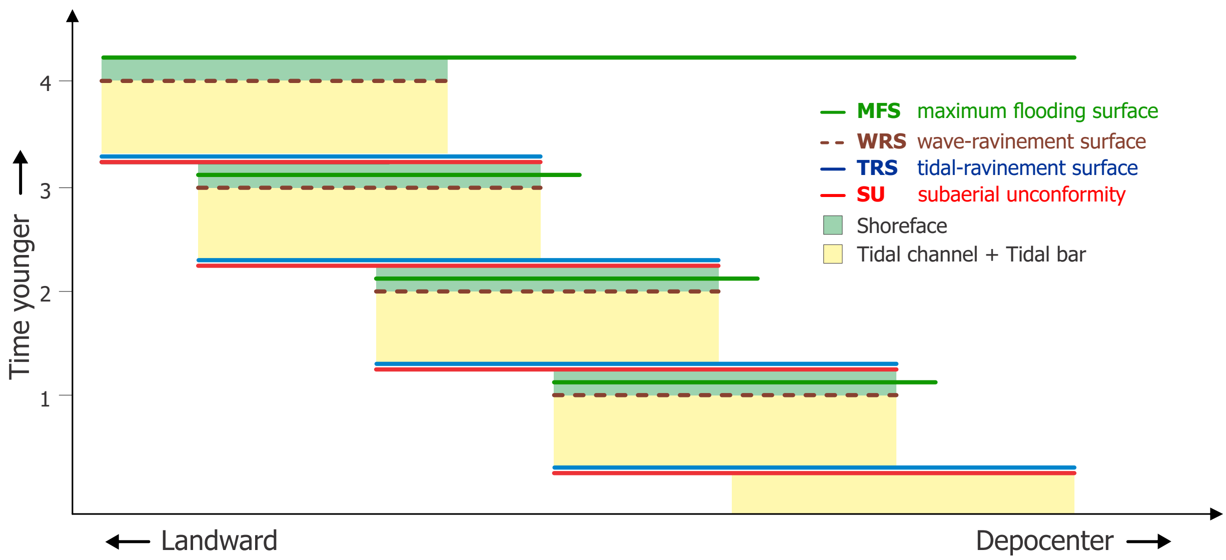

Figure 13. Schematic transgressive succession composed of tidal channels and bars overlain by shoreface strata. As the location of WRS development shifts landwards during transgression, WRS is neither connected nor superimposed by the previous surface of similar nature. Instead, they are separated by transgressive deposits. Note that high-frequency regressions materialized by SU punctuate the long-term transgressive trend.

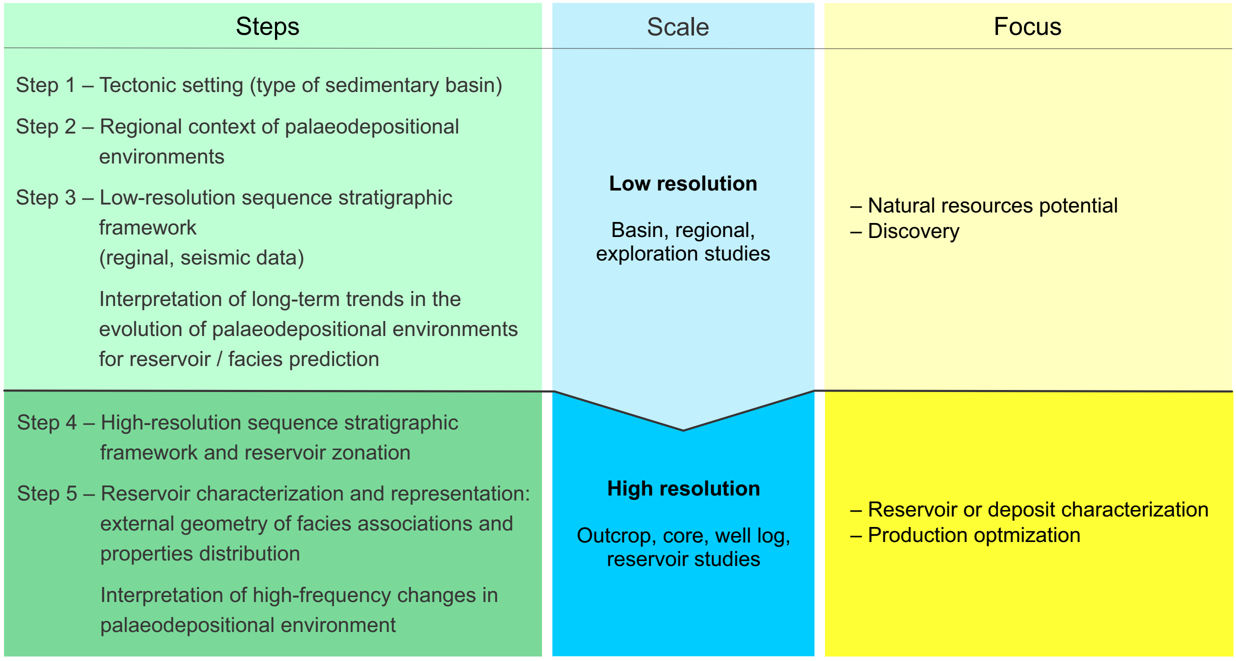

Source: modified from Magalhães *et al.* (2020).

Figure 14. The available data's scale constrains the sequence stratigraphic workflow. Note that a chronostratigraphic framework must precede facies representation on both scales.

bounding surfaces that determine their regressive or transgressive character and indicate the location of the source area and depocenter. Thus, the chronostratigraphic framework leads to detailed paleogeographic reconstruction, which allows predicting the occurrence of facies of interest beyond the control points. The stacking pattern of high-frequency sequences indicates trends that mark the boundaries of the immediately higher sequence hierarchy that, in turn, act as a constraint for the high-frequency study (Magalhães *et al.* 2020, Fragoso *et al.* 2021). Therefore, the low- and high-resolution analyses calibrate each other and improve the understanding of the stratigraphic evolution of a given interval, which has a strong positive economic impact on the outcome of exploration and production projects (Magalhães *et al.* 2020).

Support of geotechnologies on stratigraphic analysis of outcrops

The ongoing geosciences technological revolution , particularly regarding the use of digital and virtual outcrop models (DOM/VOM) and Ground Penetrating Radar (GPR) to extract 3D georeferenced geological objects, substantially improved the stratigraphic analysis of the exposed stratigraphic record (Hodgetts 2013, Howell *et al.* 2014, Buckley *et al.* 2019, Burnham and Hodgetts 2019, Marques Jr. *et al.* 2020). DOM/VOM are photorealistic 3D models of outcrops, projected in 3D as point clouds or textured meshes, possibly containing dozens of thousands of points/m^2 in a point cloud and triangles in a mesh. A texture map may have up to 270 megapixels; the derived 2D products as orthophoto mosaics and digital surface models usually have cm to mm/pixel spatial resolution. Such high-resolution 3D models are complemented by digital terrain models (DTM) built from satellite images and digital elevation models.

The Chapada Diamantina region (Brazil) provides an example of stratigraphic interpretation based on DTM and DOM/VOM. The unconformity between the Middle Espinhaço I and II sequences (Magalhães *et al.* 2016) was mapped with high accuracy on the cliffs surrounding the Pai Inácio hill area (Fig. 15). Some of these locations are inaccessible, but facies analysis in adjacent areas covered by the DTM supports this interpretation. ME-I and ME-II represent first-order sequences (i.e. basin-fill during distinct geotectonic evolution, according to Catuneanu 2006). These sequences stand for two sag superimposed basins separated by a hiatus of approximately 100 Ma (Magalhães *et al.* 2016).

GPR is a widely used method for near-surface geological investigation (Annan 2009) to image features with variable resolution and penetration depth (Jol 1995), such as the geometry of sand bodies, as well as the correlation and quantification of sedimentary structures (Bristow and Jol, 2003), facies architecture and high-frequency stratigraphic framework (Magalhães *et al.* 2017, 2021). GPR data from outcrops analogs of hydrocarbon reservoir have been used since the 1990s (Thompson *et al.* 1995) and have turned into the chief near-surface investigation method in different geological settings (Souza *et al.* 2018, Dougherty *et al.* 2019, Leandro *et al.* 2019, Bermejo *et al.* 2020, Medina *et al.* 2020).

The integration of DOM/VOM and GPR of laterally and vertically wide exposed strata is revolutionizing the identification of stacking patterns and stratigraphic surfaces in both field and laboratory. Depending on the resolution of the DOM/VOM and GPR products, the position of a facies contact, or a sequence stratigraphic surface may be determined in 3D models as a point, line, or digital surface object. The use of such methods during the stratigraphic analysis of outcrops enhances and optimizes information acquisition and allows

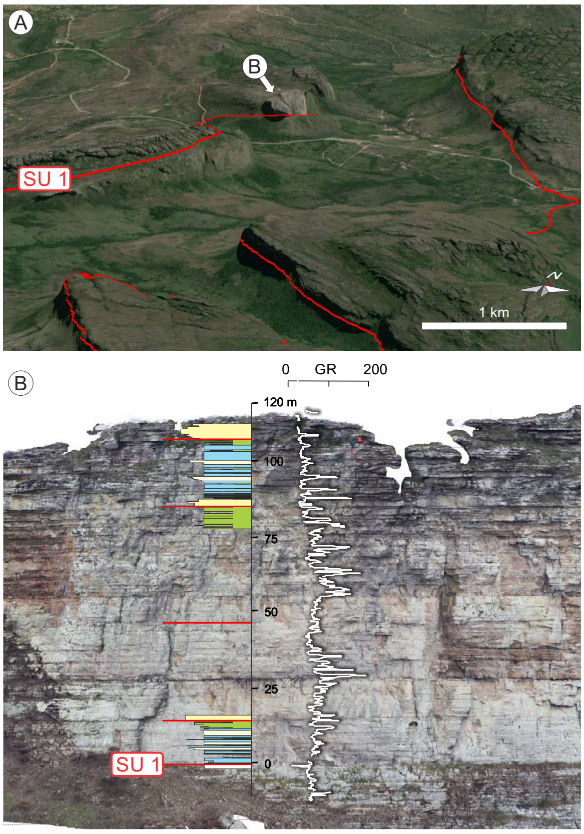

Figure 15. (A) Orthographic projection from DTM at the Pai Inácio anticline (built from Also Palsar digital elevation model overlaid by CNES Airbus image), Chapada Diamantina Basin, northeastern Brazil. The SU1 unconformity, between Mesoproterozoic Middle Espinhaço I and II sequences, is mapped along the cliffs. (B) Low-frequency subaerial unconformities identified on the orthographic projection from DOM/VOM (built from aerial images acquired from a helicopter) of the Pai Inácio hill integrated with the facies and the GR log (modified from Magalhães *et al.* 2016).

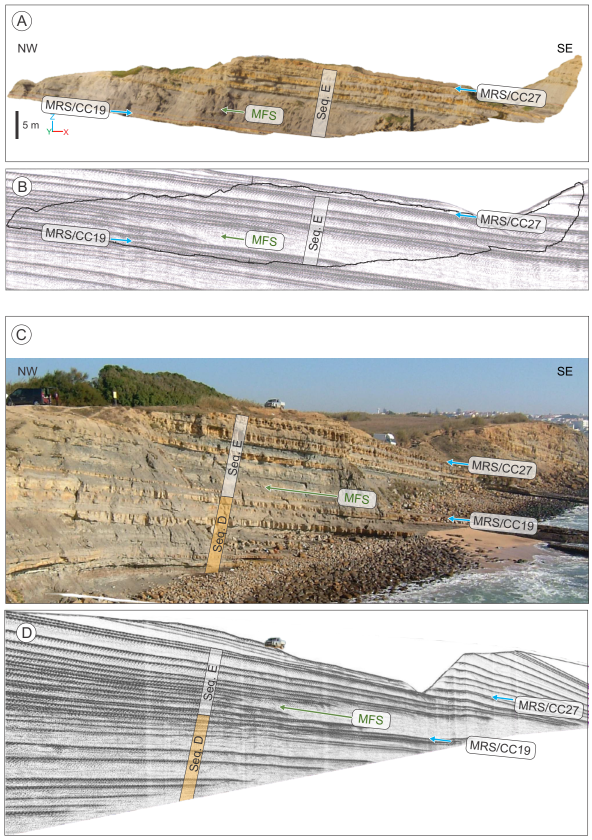

Figure 16. Medium-frequency T-R sequences from the Lusitanian Basin (Magalhães *et al.* 2021). (A) Orthophotomosaic from DOM/VOM. (B) 200 MHz synthetic GPR from the outcrop. (C) A photo from the same location in perspective. Note the muddy character of TST and the amalgamation of HST sandy and carbonate strata that prograde southwards. (D) 200 MHz synthetic GPR profile mirrors the outcrop features and recognizes distinct stacking patterns and sequence stratigraphic surfaces.

the compilation of a database of georeferenced information in 3D, thus improving the stratigraphic model building.

An example of integrating DOM/VOM and GPR to assist a stratigraphic analysis of an outcropping succession in the Lusitanian Basin was presented by Magalhães *et al.* (2021). According to the authors, the lower portion of the studied succession records sedimentation on a Middle-Jurassic ramp composing T-R high-frequency sequences (Embry and Johannessen 1992, Embry 1995) between 1 and 7 m thick. Transgressive strata comprise claystone and siltstone. Regressive deposits consist of a lagoonal carbonate and occasional upper shoreface bioturbated and hybrid sandstone. These sequences make up medium-frequency T-R sequences between 9 and 21 m thick that exhibit muddy TST and amalgamated sandy to carbonate HST strata, both characterized and mapped throughout the study area using DOM/VOM and orthophotomosaics (Fig. 16).

Application on exploration and production of natural resources

The following hypothetical example explains the economic impact of a petroleum production project based on litho- and chronostratigraphic correlation. The project aims to inject water in the well 2 reservoirs to enhance oil production from well 1 (Fig. 17). The lithostratigraphic correlation indicates that the project would be successful (Fig. 17A). However, as shown through chronostratigraphic correlation, the prograding reservoirs are not laterally connected (Fig. 17B), and therefore, the project is not recommended. The heterogeneities observed in the chronostratigraphic model can be confirmed through an outcrop analog (Fig. 17C). The lateral facies contact and shelf claystone strata, including the high-frequency MRS/MFS, promote impermeable barriers that do not allow fluid communication *between* the reservoirs. Instead, fluid flow occurs independently *through* each one of them (white arrows).

The selection of a datum is vital for a chronostratigraphic correlation. The best datum is the stratigraphic surface with the lowest diachroneity, such as the MFS and MRS. Even though all stratigraphic surfaces are diachronous to some extent, the MFS is a better datum because it's a conformable surface developed over large areas of the basin at the end of the transgression, when the depositional topography is the flattest (Fig. 15). The maximum regressive surface is the second-best option for a datum, especially in shallow-marine, coastal, and downstream fluvial settings (see discussion on stratigraphic surfaces in Catuneanu 2006). Regardless of the chosen datum, a

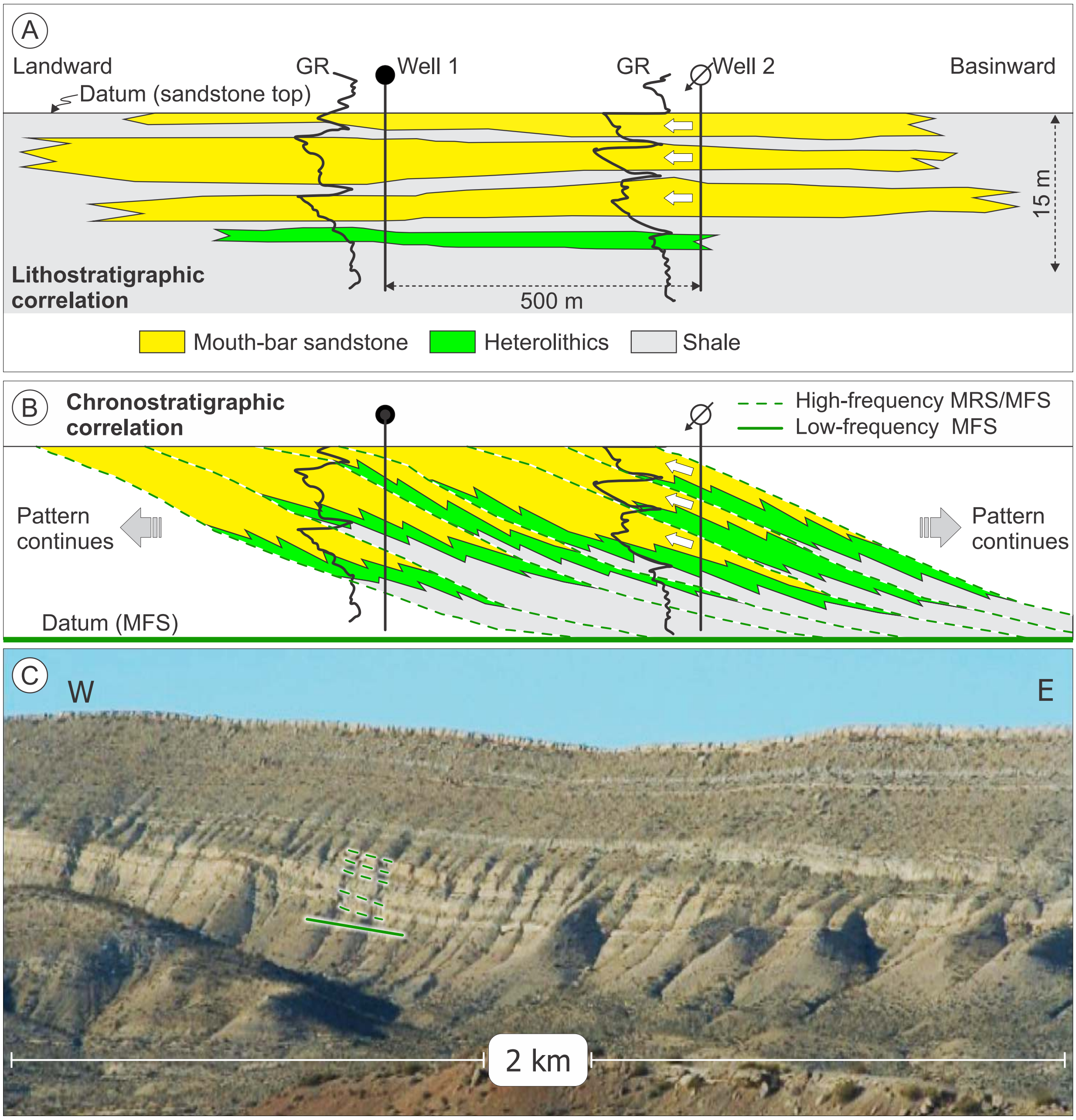

GR: gamma-ray log.

Figure 17. The lithostratigraphic correlation (A) does not represent the stacking pattern and hence, may induce poor outcomes in production project (modified from Ainsworth *et al.* 1999). The chronostratigraphic correlation (B) mirrors the appearance of a normal regression on outcrop (modified from Ainsworth *et al.* 1999) (C) and stands for the more realistic representation of reservoirs and heterogeneities. Outcrop from the Middle Jurassic Lajas Formation in Neuquén Basin Argentina (photo courtesy of Carlos Arregui).

chronostratigraphic cross-section must adequately represent the changes in depositional trends to allow a realistic view of spatial and areal distribution of the natural resources or the reservoirs. Moreover, paleogeographic reconstruction can better address the sedimentary evolution based on several chronostratigraphic cross-sections with their data associated with high-frequency sequence stratigraphic surfaces.

Chronostratigraphic correlation: examples based on rock, well log, and seismic data

The Albian succession of the Potiguar Basin in Brazil provides an example of a low-resolution seismic-scale chronostratigraphic correlation between continental and marine strata (Melo *et al.* 2020). The succession is part of the drift phase and holds the basin's primary oil-bearing unit. In this study, the authors integrated seismic, well log and rock data to individualize sequences and systems tracts recognized in depositional dip-oriented seismic lines. Based on core description, depositional sequence 1 comprises fluvial strata landward from well 17 and marine (siliciclastic and carbonate) deposits basinward from well 18 (Fig. 18).

According to Melo *et al.* (2020), SU1 erodes post-rift Aptian deposits and the pre-Cambrian basement landward. Basinwards, SU1 connects to correlative conformity (CC1) at the top of the Aptian interval. MRS is marked on top of a high-energy braided fluvial strata overlain by meandering

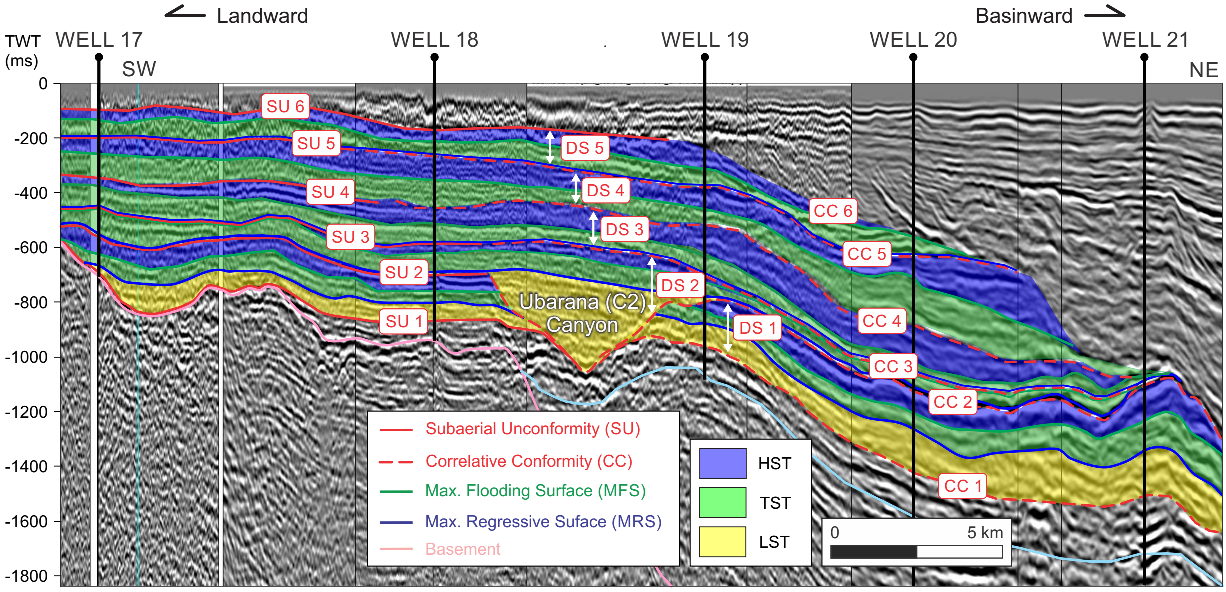

Figure 18. The dip-oriented seismic line shows depositional sequences 1 to 5 from Albian to Campanian in the Potiguar Basin (Melo *et al.* 2020). Depositional sequence 1 (DS 1) is entirely fluvial landward from well 17 and marine basinward from well 18.

fluvial deposits landwards, or on top of a regressive transitional to marine strata basinward (i.e. Açu Formation). The TST shows onlap stratal termination over MRS in the marine portion of the basin and is represented by the deep-water carbonates (Ponta do Mel Formation; Tibana and Terra 1981, Terra 1990). The HST consists of fluvial to coastal deposits that grade basinward to the mixed and carbonate strata (i.e. the lithostratigraphic transitional contact between the Açu and Ponta do Mel formations, Fig. 19).

Upon closer examination, the seismic line between wells 17 and 18 shows distinct seismic facies associated with depositional systems in each systems tract (Fig. 20). The fluvial strata display channel-like features and transitional deposits exhibit parallel reflectors. Zigzag lines indicate the depositional trend and lateral facies contact in each system tract. Hence, the zigzag lines highlight the normal regression of braided fluvial, coastal and siliciclastic marine systems during LST, the transgressive aggradational and backstepping pattern of marine carbonates, estuarine, and meandering fluvial systems, as well as the normal regression of meandering fluvial, coastal, and shallow-marine carbonate systems throughout the HST (Fig. 20). The higher thickness of the carbonate when compared to its clastic counterparts suggests carbonate keep-up due to increased accommodation triggered by sin-depositional faults (Fig. 21). The top of the HST exhibits epigenic karstic features on shallow-water carbonates and fluvial to coastal strata truncation. Intense percolation of meteoric water through originally porous shallow-water facies completely cemented the carbonate facies (Fig. 19; Terra 1990).

The low-resolution chronostratigraphic correlation and zigzag lines indicate the depositional systems's major domains in each systems tract. As different sedimentary processes operated in each domain, they generated distinct depositional facies with particular petrophysical properties. Given the low porosity of the carbonate facies due to cementation, the best exploratory targets are the sandstone reservoirs from the continental to transitional settings. Therefore, defining these domains is not a strictly academic matter but an essential guide to new data acquisition strategy, well drilling and 3D geologic modeling to support exploration and production development projects (e.g. Magalhães *et al.* 2020).

Further chronostratigraphic refinement must be carried out if data are available. According to Melo *et al.* (2020), the TST of depositional sequence 2 was subdivided into fourth-order sequences that stand for the reservoir zones and are composed of transgressive meandering fluvial deposits. As shown in the GR logs, fining-upward trends coupled with the upward increase of clay content indicate a high-frequency transgressive stacking pattern (Fig. 22). The top of the palaeosol from overbank deposits marks a high-frequency SU, which is superimposed by MRS located at the base of the transgressive meandering fluvial strata.

Sequence stratigraphy and diagenetic evolution in carbonates

The initial porosity of any carbonate rock can be entirely transformed by near surface and sub-surface diagenetic processes (Fig. 23). Therefore, an original porous carbonate deposit may not turn into an oil reservoir, just as a non-porous rock can become an excellent reservoir through diagenesis.

Feazel and Schatzinger (1985) listed the main factors that destroy or preserve porosity in carbonate rocks (Fig. 24). Some factors such as framework rigidity, mineralogical stability, burial history, abnormal pressure and oil entry are independent of sequence stratigraphy. However, zone boundaries identified through HRSS promote permeability barriers that play a significant role in preserving depositional porosity. These barriers prevent the circulation of cementing fluids in the porous space, which is one of the main causes in the loss of porosity. The best situation occurs when porous carbonates are overlain by evaporites or other impermeable facies culminating in the top of a high-frequency regressive tract or by fine facies such as mudstones or shales from a transgressive tract (Fig. 25). Thus, sequence stratigraphy allows the understanding of many diagenetic imprints in carbonate, such as:

- how primary porosities can be preserved.

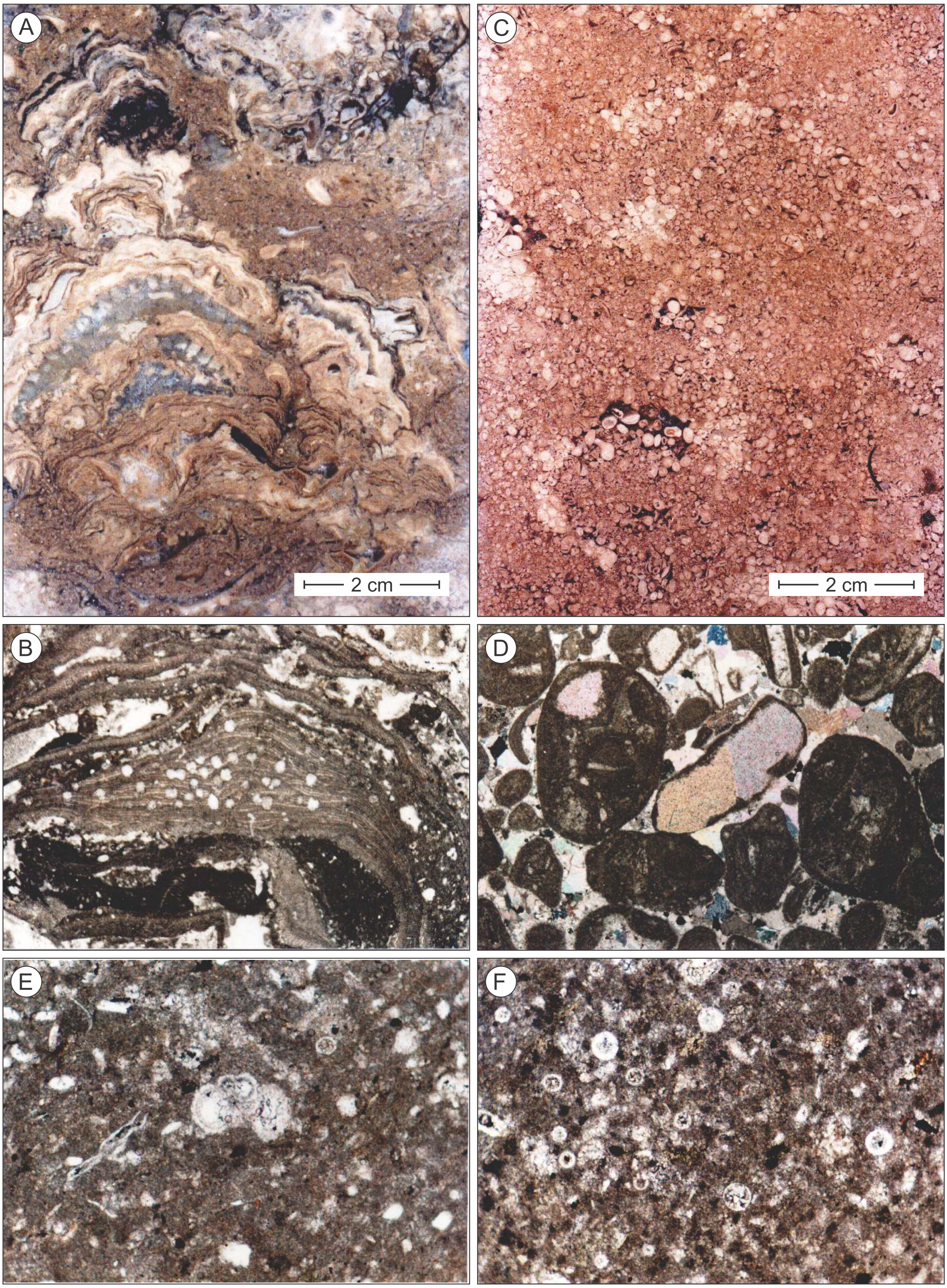

Figure 19. Aspects of the carbonate facies from a core slice to a thin-section in the Ponta do Mel Formation (Terra 1990). (A) Coralgal boundstone and (B) plane-polarized light, photo horizontal axis = 4.5 mm. (C) Oncolitic grainstone and (D) cross-polarized light, photo horizontal axis = 4.5 mm. (E) Mudstone with planktonic foraminifers (*Favusella Washitensis*). Plane-polarized light, photo horizontal axis = 0.9 mm. (F) Mudstone with calcispheres on the right. Plane-polarized light, photo horizontal axis = 1.1 mm. Note that the carbonate facies are highly cemented. Regarding the location, see Fig. 21.

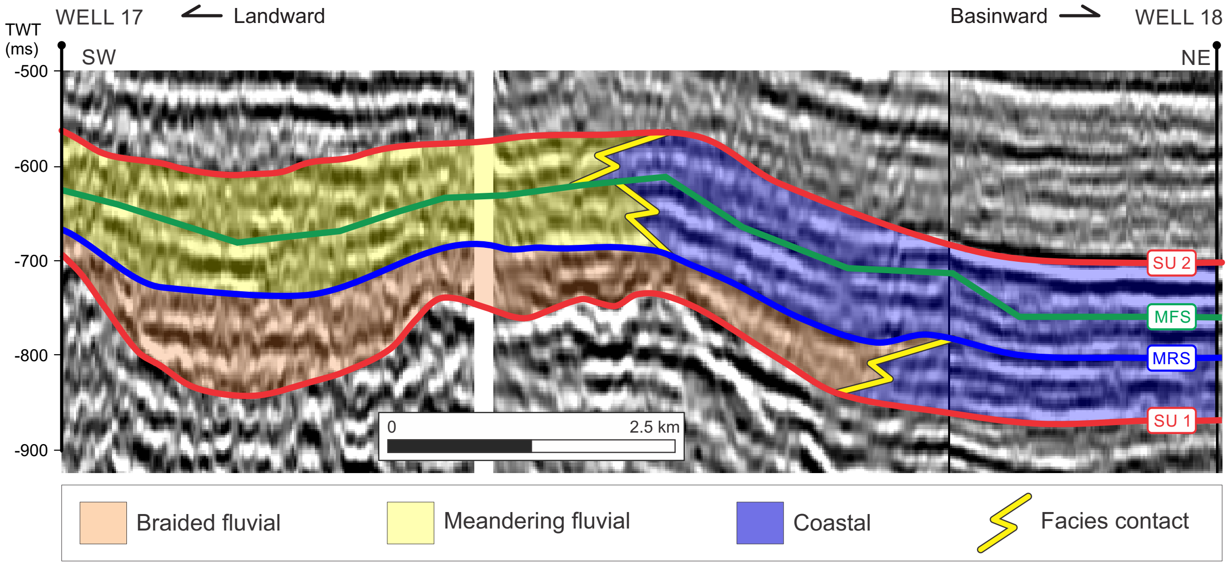

Figure 20. A close view from a seismic line between wells 17 and 18 shows distinct seismic facies from LST, TST, and HST from depositional sequence 1. The zigzag lines indicate the lateral facies contacts between depositional systems that compose each systems tract. Seismic line from Melo *et al.* (2020).

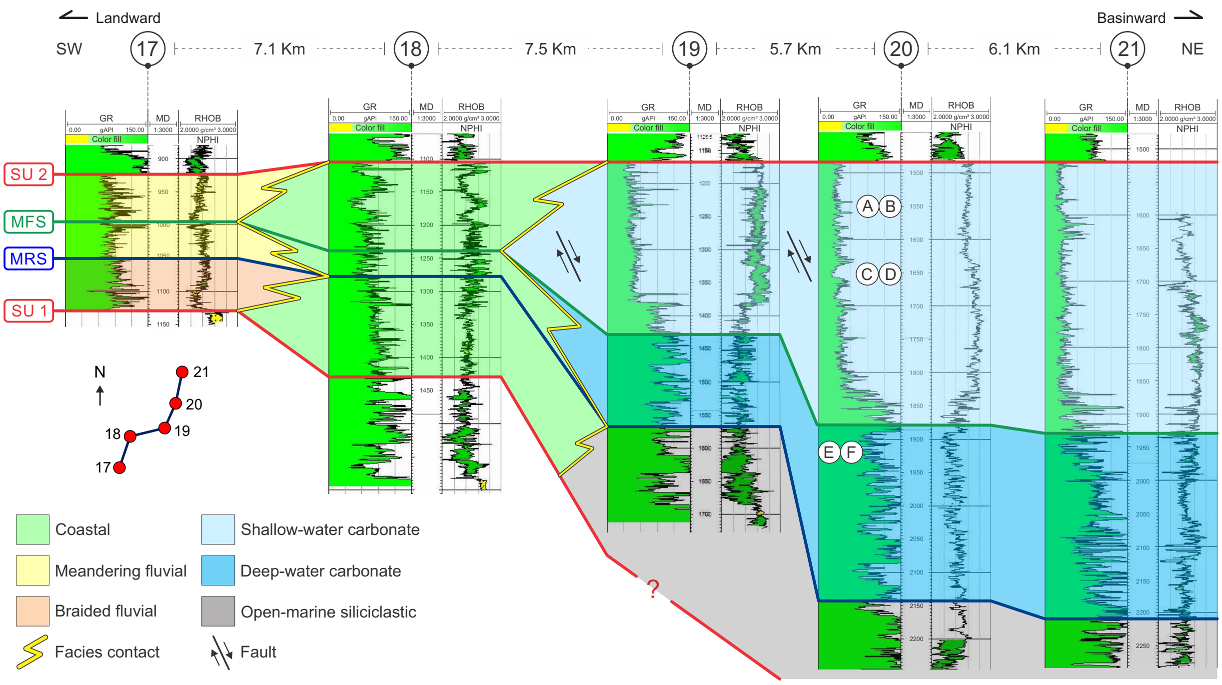

Figure 21. Low-resolution chronostratigraphic cross-section based on well logs calibrated with seismic and core data. SU2 was chosen as datum since it closely relates to the paleodepositional surface at the end of HST. The larger carbonate thickness indicates keep-up of the platform due to accommodation created by sin-depositional faults. Letters indicate the location of the photos shown in Fig. 17.

- how dissolution can generate subaerial karstification.
- how near-surface dolomitization processes can completely modify the permo-porous characteristics.
- how the sub-surface diagenesis can be influenced by impermeable (seal) layers, favoring dissolution and dolomitization by ascending, hydrothermal fluids.

In order to understand the diagenetic evolution of marine carbonates, an example of HRSS application was presented by Correa *et al.* (2013) in the Oligocene-Miocene interval of an offshore oil field in the Campos Basin, Brazil. These deposits correspond to a long-term regression (second order) that occurs along all Brazilian East margin basins (Asmus and Porto 1980, Bruhn *et al.* 2003, 2017). According to the authors, the succession is mainly composed of red algae-rich wackestones, packstones, rudstones, and bindstones, which comprise different facies associations in backreef, reef, and forereef settings (Fig. 26). The study presented an integration of seismic attributes extracted from high-resolution seismic data, 24 wells logs, as well as continuous core data. Data integration allowed the definition of four third-order stratigraphic sequences, in which HSTs' clinoforms sets are interpreted in seismic data (Fig. 27). Further stratigraphic refinement identified fourth-order sequences that constrained the facies distribution and

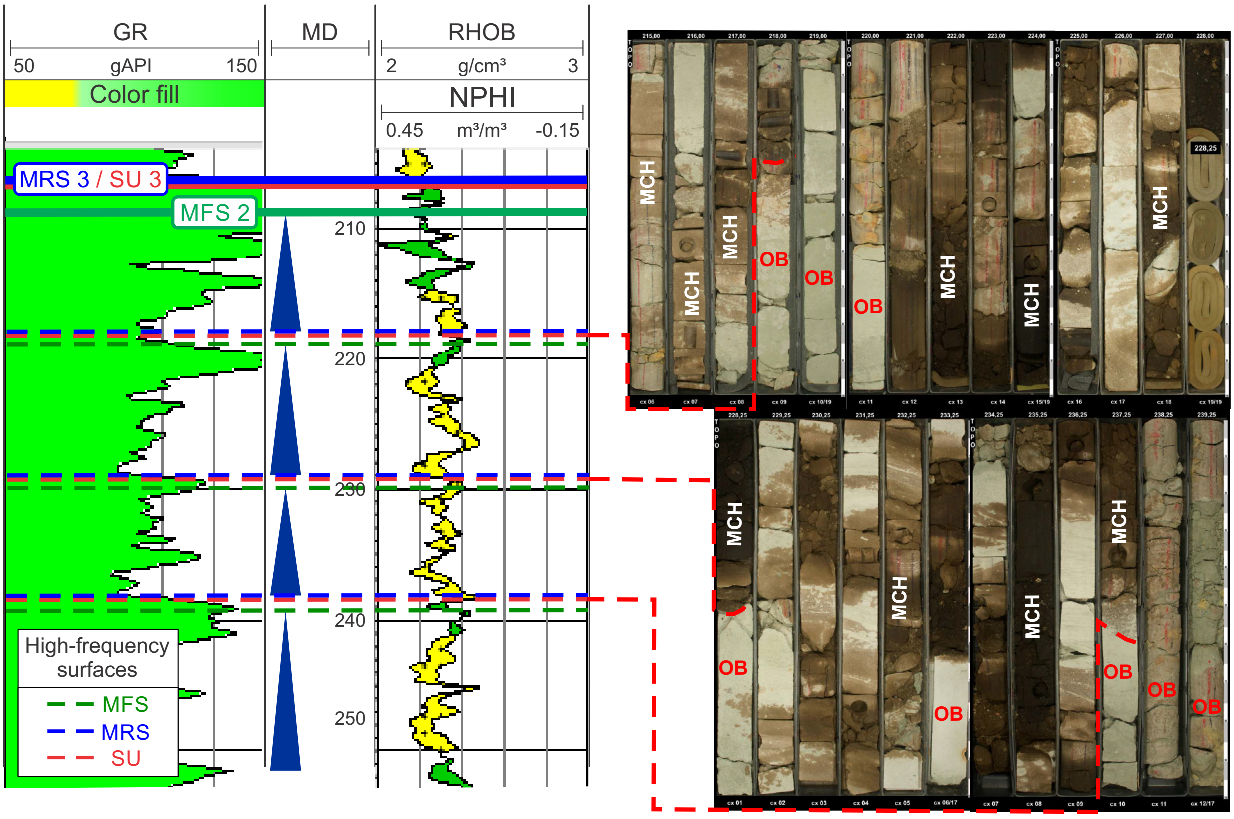

Figure 22. High-frequency stratigraphic sequences compose a third order TST (topped by MFS 2) and account for reservoir zonation. SU placed at the top of paleosol intervals from overbank deposits (OB) is superimposed by MRS at the base of the transgressive meandering fluvial strata (MCH; Melo *et al.* 2020).

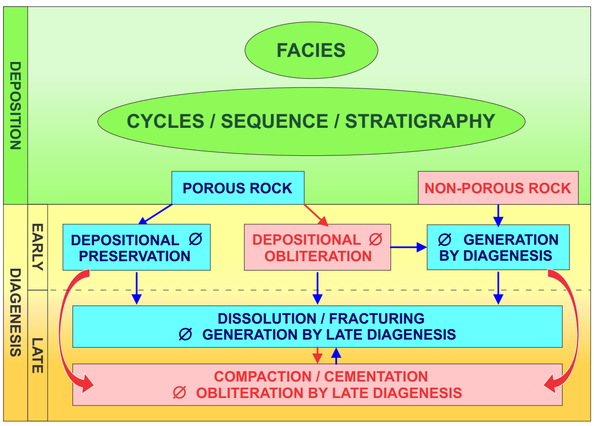

Figure 23. Permo-porous system of carbonate reservoirs.

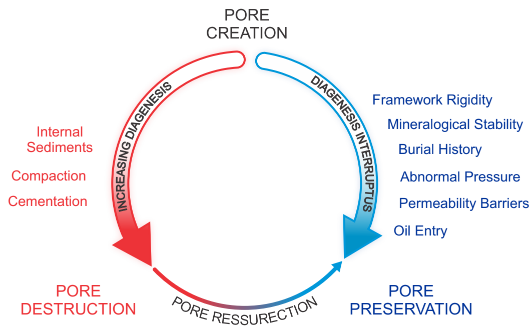

Source: modified from Feazel and Schatzinger (1985).

Figure 24. The presence of porosity in subsurface carbonates depends on a delicate balance between pore destruction and pore preservation mechanisms.

related petrophysical properties (e.g. porosity, permeability). Vuggy carbonate facies with very high porosity (> 40%) and permeability (> 50D) were recognized in cores, well logs and an extended well test. These features were interpreted as the result of epigenetic karstification associated with subaerial unconformities and sub-vertical fracture corridors composing super-k layers (Fig. 28). Therefore, the high-resolution stratigraphic framework enabled the association of the diagenetic events related to subaerial exposure surfaces, explaining the exceptional porosity and permeability found in the field.

The Jurassic carbonate succession of Smackover and Bucker formations is an example of changes in depositional porosity by diagenesis processes related to different systems tracts (Moore 2010). Sequence II's depositional history begins with the sedimentation of aragonitic-oolitic grainstones during HST (Fig. 29A). The mineralogy of inorganic carbonate components has changed throughout the geological time, and the predominant aragonitic seas during much of the Jurassic (Dickson 2004) determined the oolites' composition. The photomicrograph (Fig. 29A) shows modern aragonitic oolites from the Bahamas, comparable to those deposited during the Jurassic. Aragonite is a metastable mineral dissolved or neomorphosed to the stable form of low-magnesium calcite during the diagenesis evolution. During subaerial exposure, meteoric water dissolved the aragonitic oolites and produced oomodic porosity and low-magnesium calcite cement that reduced the intergranular porosity and permeability in a complete textural

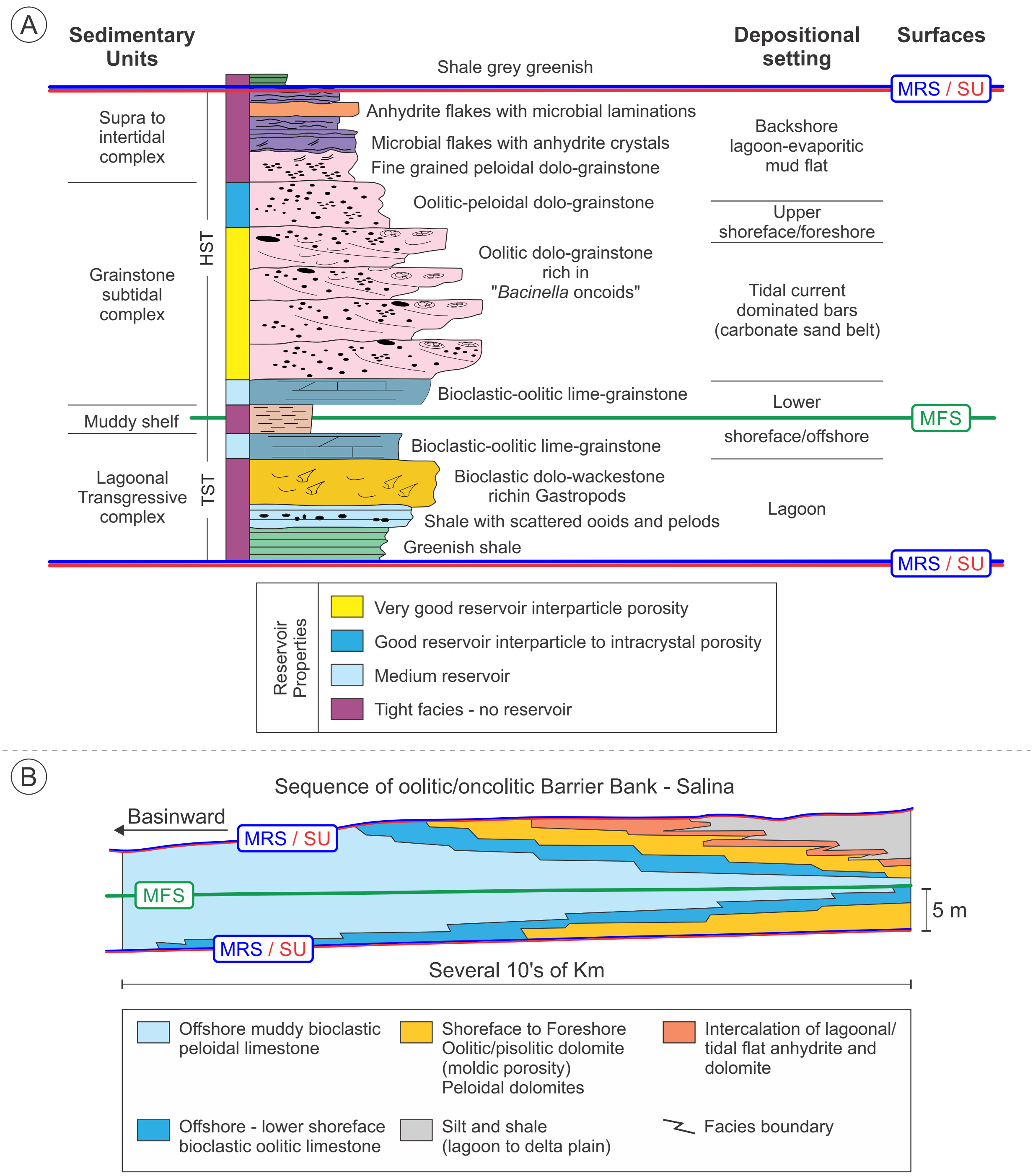

Source: modified from Eichenseer *et al.* (1999).

Figure 25. (A) Detailed facies analysis within (B) the high-resolution stratigraphic framework sequence of the Pinda Group, Kuanza Basin, Albian, offshore Angola. The best reservoirs are the regressive grainstone subtidal complex overlain by impermeable anhydrite from the supra-to intertidal complex. This impermeable seal favored the preservation of primary porosity by avoiding the circulation of cementing fluids.

inversion of the original rock. The photomicrograph (Fig. 29B) is a sample from the Bahamas where Pleistocene aragonitic oolites are exposed to undergoing dissolution through meteoric diagenesis, similar to what occurred in the Jurassic example. During TST, a near-surface seepage reflux dolomitization created intercrystal porosity that connected the oomoldic porosity, enhanced porosity and permeability, leading to a complete inversion of the depositional fabric and permo-porosity (Fig. 29C). This example of the Central Gulf Coast (USA) clearly shows how complex the processes are until a carbonate rock becomes permo-porous in the subsurface.

The importance of subsurface diagenesis to enhance porosity in carbonate rocks is a subject that has significantly evolved in recent years, mainly due to the occurrence of several high-productivity oil reservoirs at great depths. The importance of hydrothermal fluids in the dissolution of carbonates and precipitation of exotic minerals, Mississippi Valley-type (MVT) mineralizations, or even in the well-known cases of dolomitization have received a lot of attention from the oil industry, including incorporating concepts from mining (Davies and Smith Jr. 2006). Hydrothermal fluids ascend through faults and fractures that connect the sedimentary succession

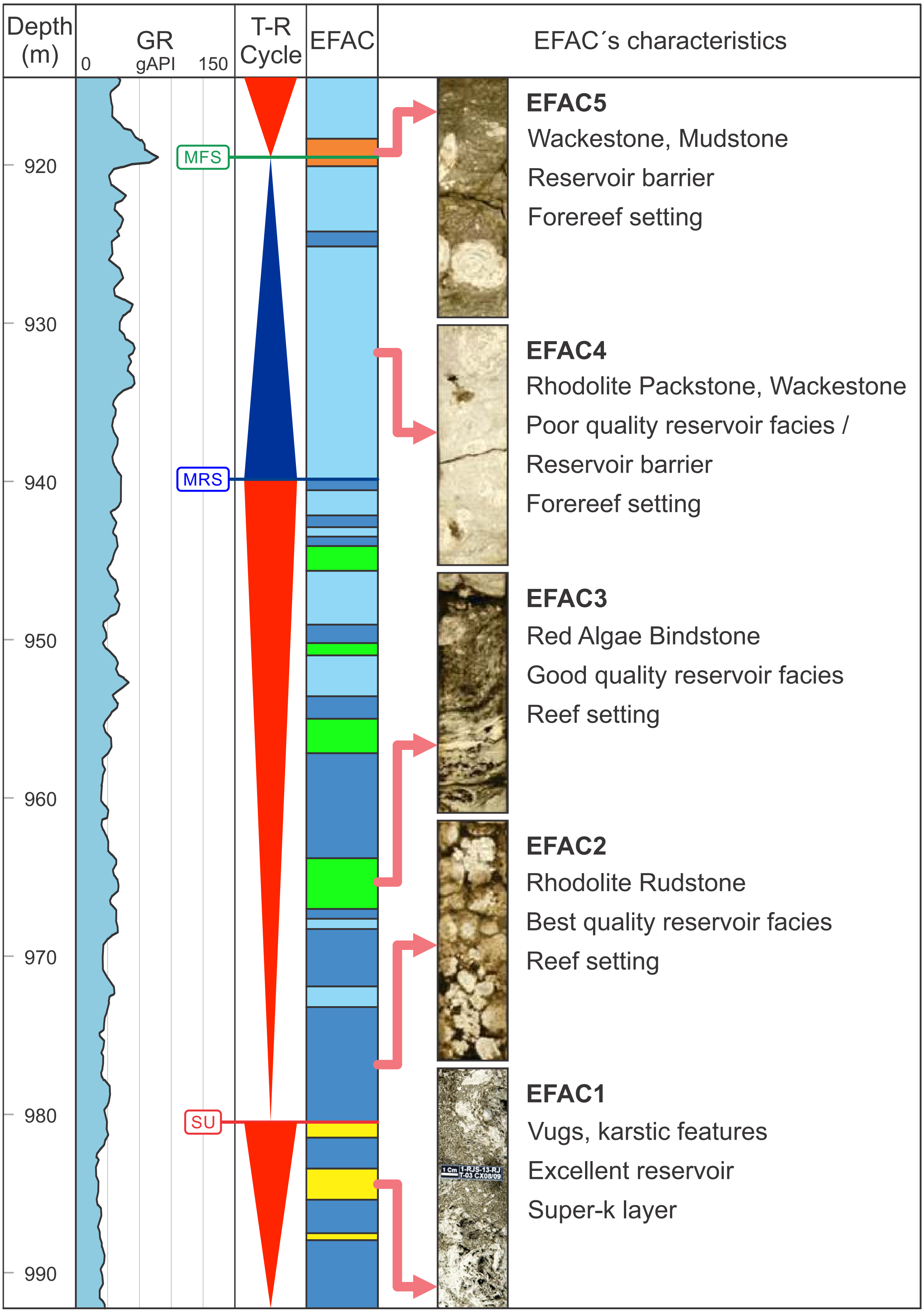

EFAC: facies associations.

Figure 26. Gama-ray log and facies associations of the Oligocene-Miocene rimmed-platform interval in the Campos Basin (Correa *et al.* 2013). Note that normal regression is punctuated by high-frequency transgressive strata.

with volcanic or basement highs where heated fluids originate. However, an indispensable factor is the occurrence of impermeable layers in the sedimentary succession that act as barriers to the ascending flow and concentrate dissolution (Davies and Smith Jr. 2006, Klimchouk 2017). The impermeable layers are mappable through HRSS and usually overlie very high productivity (i.e. super-k layer), dolomitized layers (Figs. 30 and 31).

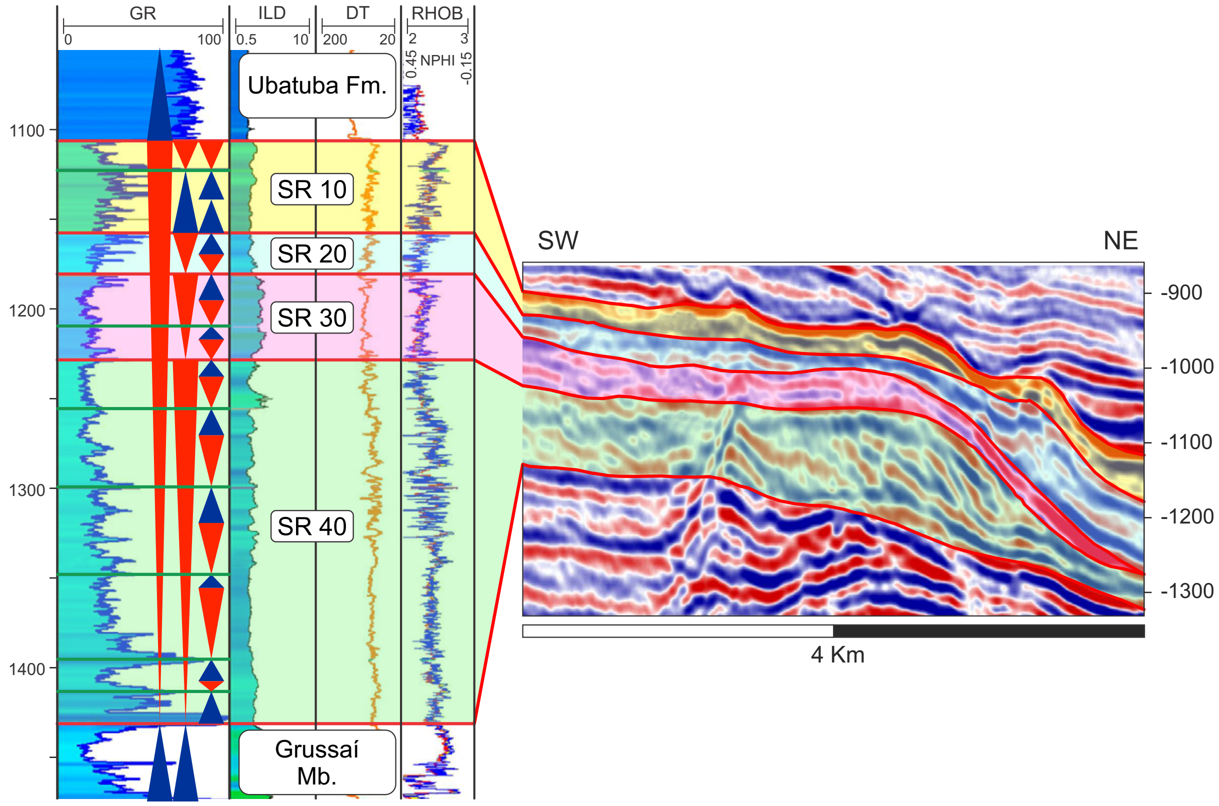

Figure 27. Nested stratigraphic architecture of the Oligocene-Miocene carbonate platform, in the Campos Basin, Brazil (Correa *et al.* 2013). The platform comprises four third-order sequences (SR 40 to SR 10) in which clinoforms sets correspond to fourth-order sequences. Hence, SR 30 was subdivided into SR 31 and SR 32, for example.

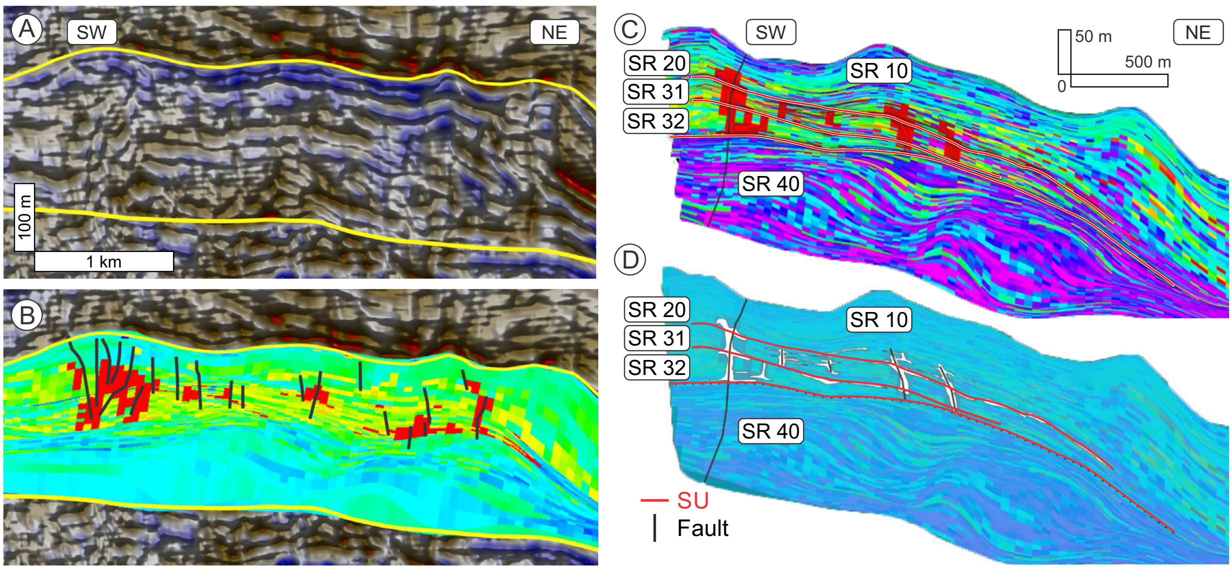

Figure 28. The integration of 3D structural (A) and facies (B) models highlights karstic features associated with natural fractures and SU on top SR 40, SR 32, (C and D) and SR 31 zones, hence promoting super-k layers (Correa *et al.* 2013).

Several mechanisms may dissolve carbonate in the subsurface such as CO_2-rich waters derived from the volcanic or magmatic activity and eventually deep mantle sources, as well as CO_2 from organic matter decarboxylation (Bögli 1980); waters containing sulfuric acid (H_2SO_4) originated when the ascending fluids pass through evaporitic rocks and incorporate the sulfate by the dissolution of anhydrite and gypsum ($CaSO_4$) and arrive loaded with H_2SO_4 in the overlying carbonate layers (Hill 1995); thermal water (mixing-corrosion), i.e. the mixture of ascending thermal waters with the formation water if the difference is higher than 4°C (Palmer 1991). Thus, the greater the temperature difference, the greater the effect of the dissolution; waters containing organic acids associated with hydrocarbon migration since the migration process from the source rock to the reservoir is preceded by organic acid fluids that dissolve carbonate rocks (Mazzullo and Harris 1992).

The complexity of the processes involved in carbonate rocks until they eventually become permo-porous reservoirs

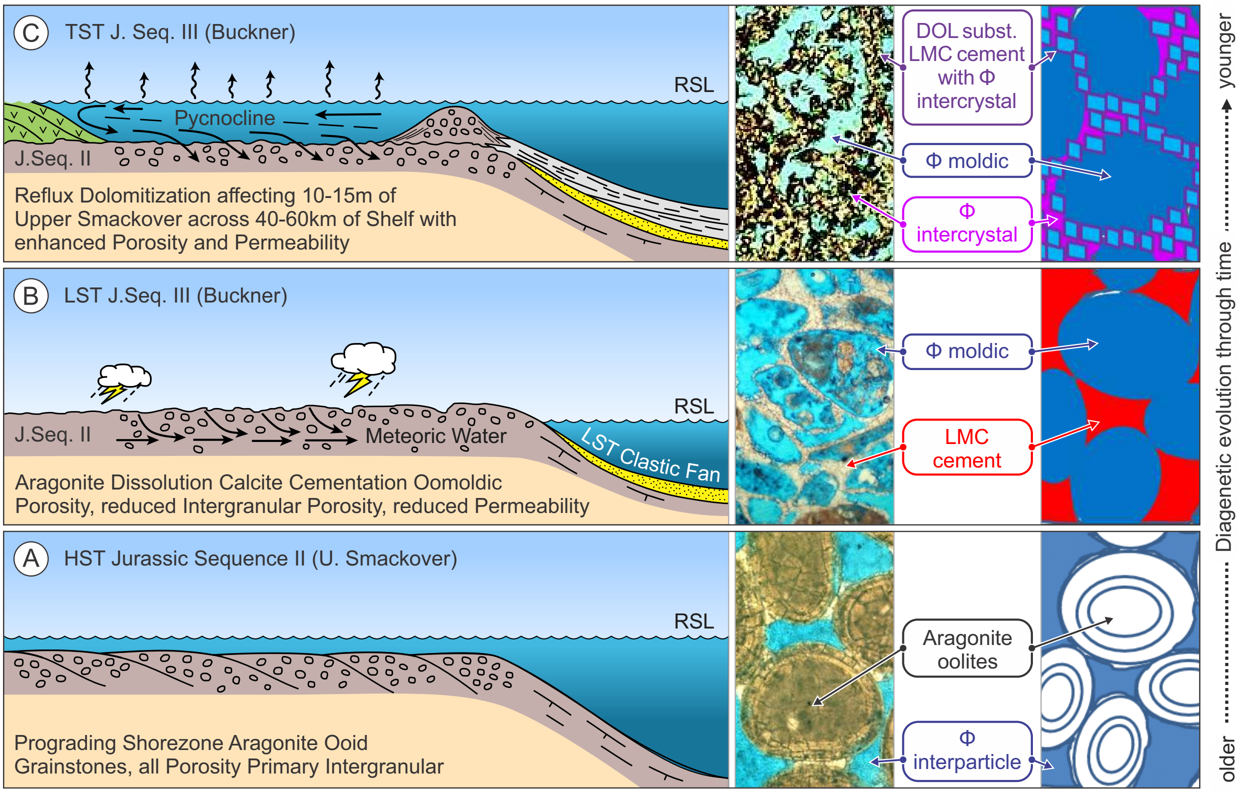

LMC: low-magnesium calcite; DOL: dolomite; ϕ: porosity; RSL: relative sea level.

Figure 29. Diagenetic evolution of a carbonate reservoir as a function of different mineralogy in systems tracts (the Smackover and Buckner formations, Oxfordian, Texas; modified from Moore 2010). Photomicrographs from the Bahamas illustrate the diagenetic events. Plane-polarized light, photo horizontal axis = 0.4 mm. Porosity types according to Choquette and Pray (1970).

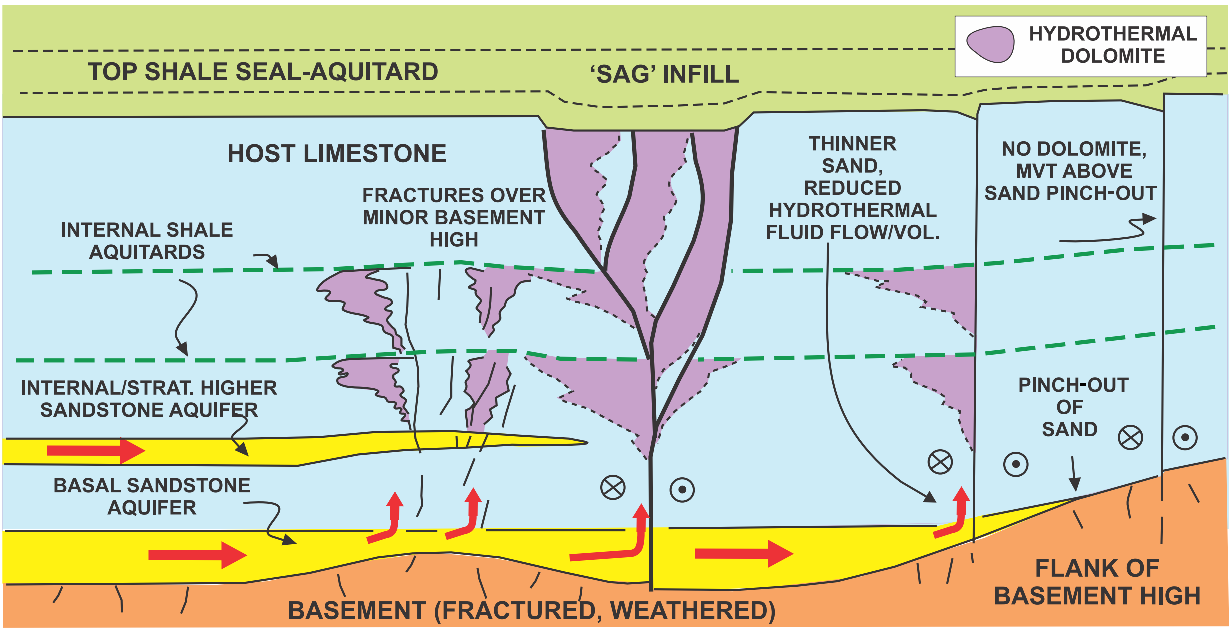

Figure 30. Schematic model for hydrothermal dolomitization based on deposits from Canada, the United States and Ireland (Davies and Smith Jr. 2006). Notice the importance of impermeable shale layers mappable through HRSS that act as a barrier to the ascending fluid flow and concentrate dolomitization.

or mineral deposits depends on how these rocks were deposited, how stratigraphic cycles were organized and how diagenesis developed near-surface and in the subsurface. A high-frequency stratigraphic framework is fundamental to integrating and understanding the interplay of these elements, hence predicting the spatial and temporal distribution of reservoirs and natural resources associated with carbonates.

Reservoir zonation and characterization and its impact on hydrocarbon production performance

One of the main applications of HRSS in the petroleum industry is reservoir zonation and characterization (Magalhães *et al.* 2020). These topics are crucial for 3D geological and fluid flow models that guide reservoir management, forecast

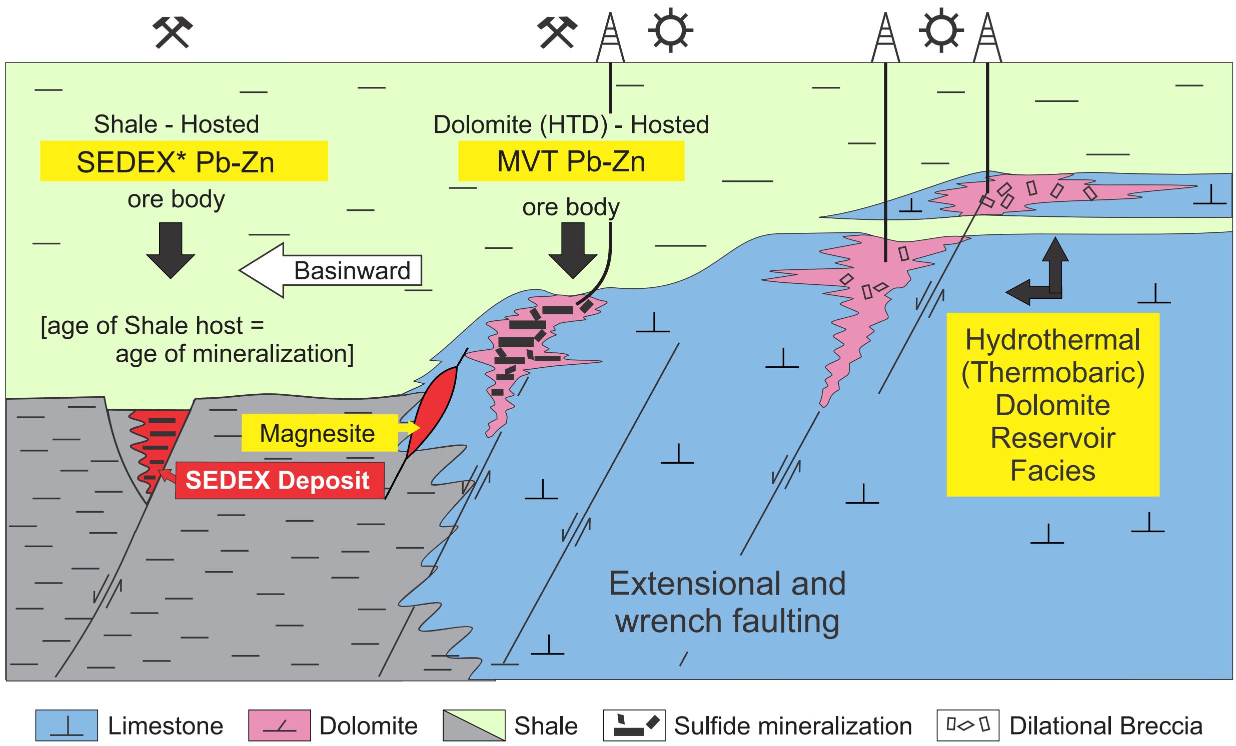

Figure 31. Schematic model representing hydrothermal mineralization (SEDEX and MVT) and hydrothermal dolomite reservoir facies in sedimentary successions (Davies and Smith Jr. 2006). Note the importance of an impermeable seal overlying all types of mineralization triggered by ascending fluids.

and optimize production, and increase the ultimate recovery factor. These models support production development projects in greenfields (i.e. new fields) and workover operations in brownfields (i.e. mature fields) that usually increase production and mark a new phase of field rejuvenation.

Fundamentally, well type (e.g. vertical, highly-deviated, or horizontal), well spacing, and production strategies in any oil field depend on the reservoir's lateral and vertical connectivity(-Fig. 15). The reservoir zonation constrains the vertical connectivity, whereas the lateral connectivity depends on facies contact between adjacent architectural elements within the zone.

Multi-layered and laterally disconnected reservoirs are common in many oil fields, and their characterization and modeling can benefit from HRSS analysis. Fluvial, mixed, and shallow-marine deposits provide some examples of this reservoir type (e.g. Torres *et al.* 2012, Magalhães *et al.* 2016). Multi-layered and laterally disconnected reservoirs exhibit flash oil production that reaches a peak and declines sharply. As the water rate (BSW) increases, water replaces oil production and many wells are needed in order to drain the zone due to poor reservoir connectivity (Fig. 32). There is a good chance of oil remaining in open zones and undrained disconnected reservoirs (Magalhães *et al.* 2020). Thus, infill drilling and secondary recovery (Improved Oil Recovery – IOR) projects may rejuvenate the field. Only after the final rejuvenation stage, Enhanced Oil Recovery (EOR) projects may be carefully considered as the last attempt to produce the residual oil. The fluid flow and water uprising through this kind of reservoir are quite different from thicker, less heterogeneous reservoirs (Fig. 33). Less heterogeneous reservoirs show relatively good lateral connections that prevent depletion, and hence typical oil production increases sharply toward a plateau, before declining abruptly. A limited number of production wells is sufficient as the water quickly replaces oil production, and eventually, there is no residual oil in the zone. Therefore, neither IOR nor EOR projects are needed.

The establishment of a high-resolution reservoir zonation may clarify some common-sense beliefs such as the high potential for oil production through horizontal wells, water coning, and tilted oil/water contact. In thick, less heterogeneous reservoirs (Fig. 33), a horizontal well drilled in the early production stage would partially drain a single zone until water floods. The residual oil above the horizontal well would be trapped in the upper portion of the zone and no longer in production. Moreover, other zones would remain undrained. In multi-layered and laterally disconnected reservoirs (Fig. 32), a horizontal well drilled in the early stage of production must consider significant uncertainties about lateral reservoir connectivity. The decision to drill a horizontal well in a mature oil field — when numerous wells have been drilled, and some zones have been drained must consider that the original fluid contacts would have moved through the water uprising due to production. In this case, a horizontal well would cross at least one water-saturated zone, and hence water would flood the well and significantly reduce oil production. Thus, a decision to drill a horizontal well must consider the high-resolution

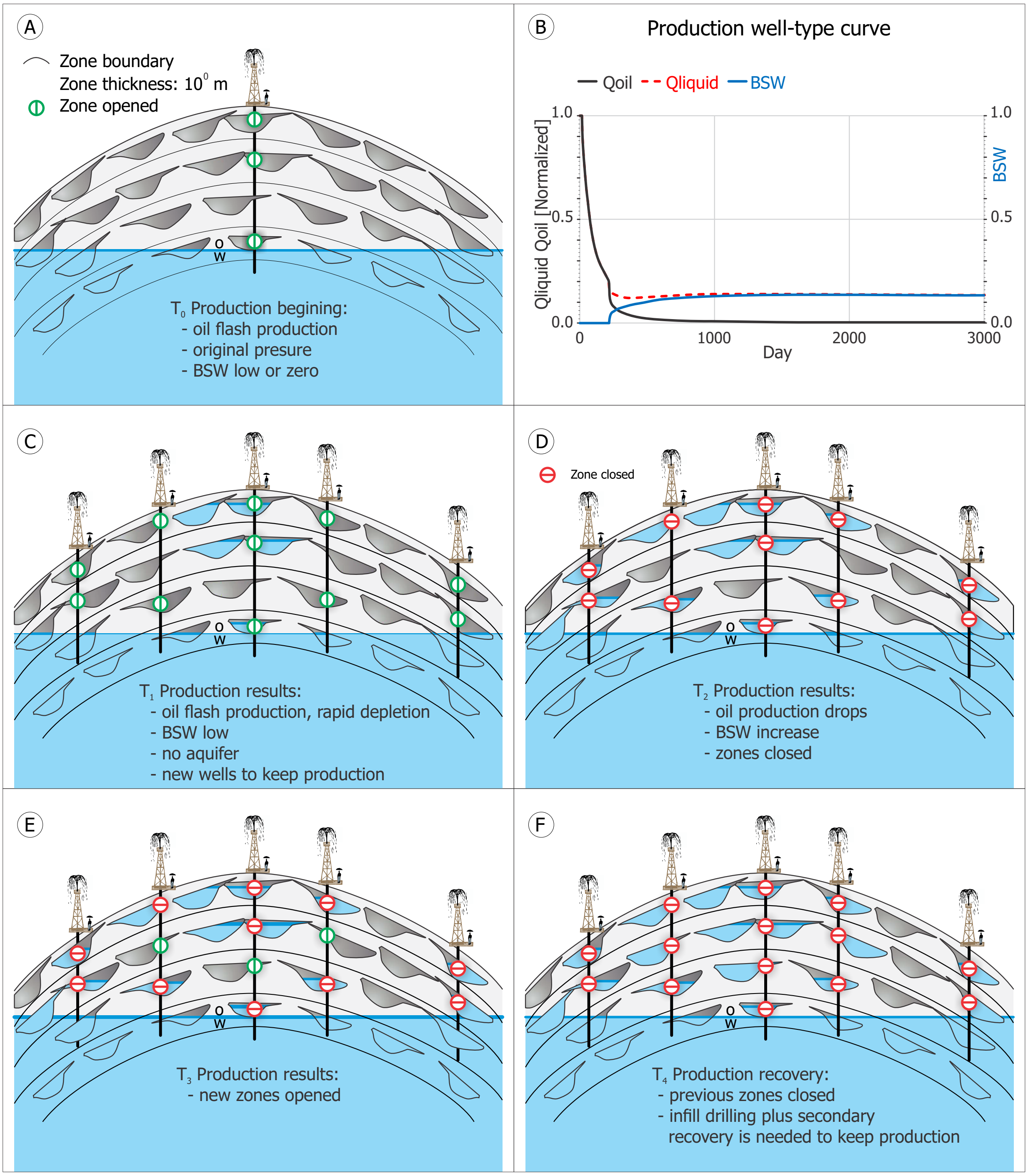

Qoil: oil rate; Qliquid: liquid (oil + water) rate.

Figure 32. Schematic representation of a thin, highly layered, and laterally disconnected reservoir (e.g. meandering fluvial, tidal bars, estuarine, coastal, and shallow-marine carbonate). It is the case of high-frequency transgressive/highstand intervals within a lower-order transgressive systems tract. Note that the reservoir width is smaller than well spacing. Black lines represent zone boundaries. (A) Discovery of the field in a hypothetical anticline. Some zones are opened to production. (B) Production well-type curve with net-to-gross (NTG) = 20%. Oil production is flash, and the water cut is low due to abrupt depletion. (C) These factors support well-planning and spacing, and hence a large number of wells (within a small space) are drilled in order to optimize production. BSW is low and starts rising. (D) As oil production declines, BSW increases, pressure drops, and many zones are closed (the blue color in the produced reservoirs means pressure depletion and water invasion). (E) New zones are opened. (F) Zones closed. There is a good chance of residual oil. Infill drilling and water injection are needed in order to rejuvenate the field.

chronostratigraphic framework since it allows for a realistic view of the spatial distribution and heterogeneities of the reservoirs.

An example of a horizontal well drilled in a multi-layered reservoir is the onshore oil field in southwestern Abu Dhabi, United Arab Emirates (UAE). The field produces from the prolific Barremian Kharaib Formation and is structurally described as a slightly elongated low relief structure with the NNE-SSE trend located between two giant fields (Torres *et al.* 2017). The Upper Kharaib reservoir comprises skeletal peloid wackestone-packstone in the lower portion, thin layers of algal, skeletal, peloid floatstone-boundstone in the middle, and skeletal peloid packstone interbedded with a good quality

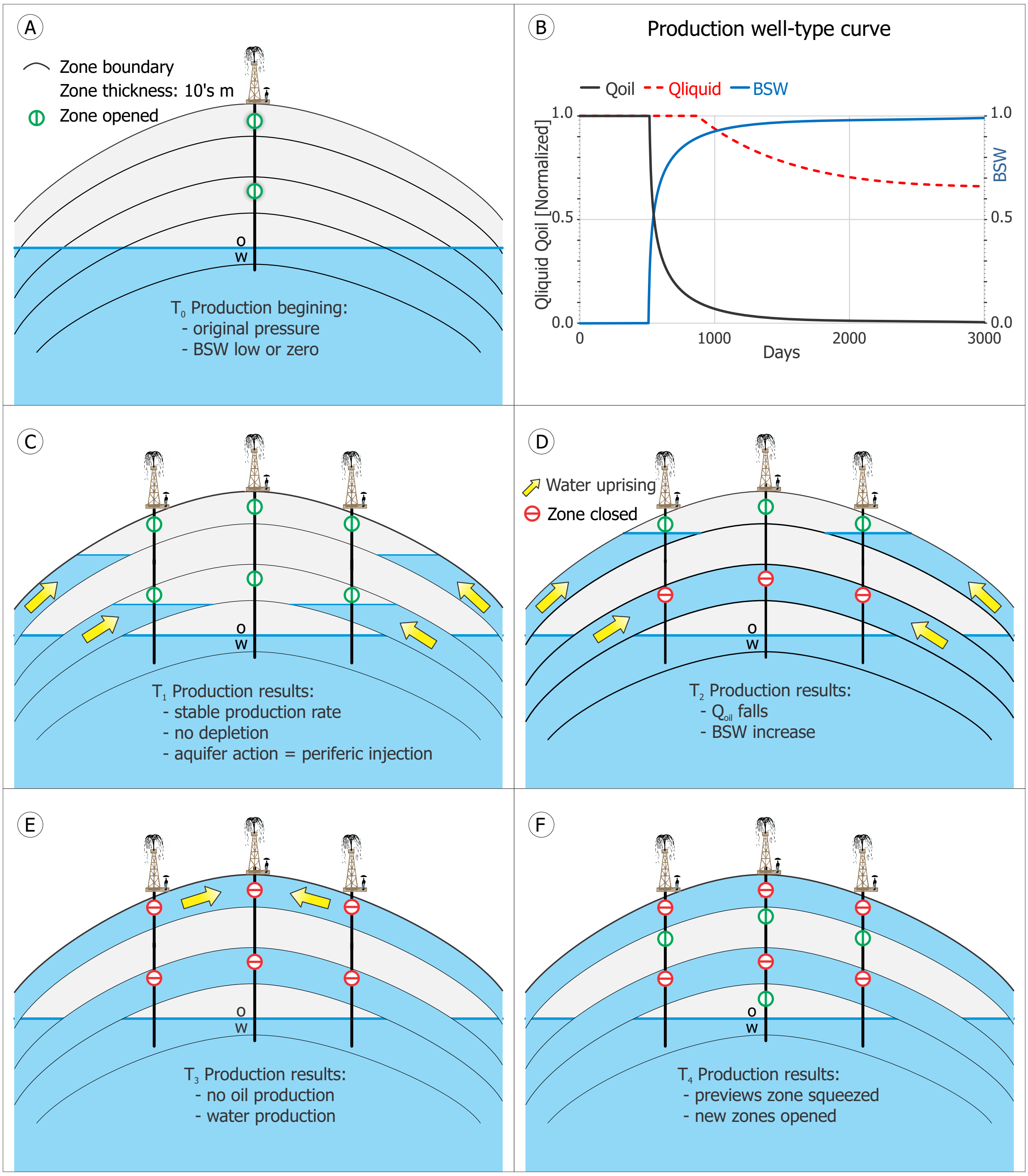

Figure 33. Schematic representation of the 10m thick, less heterogeneous, and laterally connected reservoirs (e.g. braided fluvial and eolian sand sheets, or when architectural element dimensions are more extensive than well spacing). It is the case of high-frequency lowstand/transgressive intervals within a lower-order lowstand systems tract. Black lines represent zone boundaries. (A) Discovery of the field in a hypothetical anticline. Some zones are opened to production. (B) Production well type curve. The production rate remains constant up until the first signal of an increase in BSW. Reservoir pressure remains constant due to the active aquifer. (C) These factors support well-planning and spacing, and hence a small number of wells (large spacing) are drilled to optimize production. (D) As BSW increases, water replaces oil, and (E) the opened zones are completely drained. (F) Previous zones are squeezed and new ones are opened to production. Ultimately, wells are closed, and no residual oil remains. Infill drilling and secondary recovery are unnecessary.

grainstone/rudstone reservoir in the upper portion. The reservoir was deposited in moderate- to high-energy shallow water on a broad eastward dipping ramp. Oil production started in 2013 with vertical/slanted and dedicated horizontal producer wells with support from peripheral vertical water injectors and assuming that the reservoir was comprised of only one flow unit. After four years of production, the BSW increased as reservoir pressure decreased, and some wells were closed.

A HRSS framework was established, supported by facies analysis from 14 cored wells and geophysical and reservoir saturation logs. The complete Barremian third-order sequence was further subdivided into fourth-order sequences (Fig. 34). The fourth-order sequences are 2-4 m thick and demonstrated a good correlation with petrophysical properties. Regressive facies associations were deposited in medium- to high-energy settings and exhibited good to excellent permeability. Conversely, transgressive facies associations were deposited in low-energy environments and showed very low permeability, promoting vertical fluid flow barriers. A horizontal well drilled in the upper zone confirmed this vertical compartmentalization and a new production zone whose production rate is triple the amount observed in the other wells in the field (Torres *et al.* 2017).

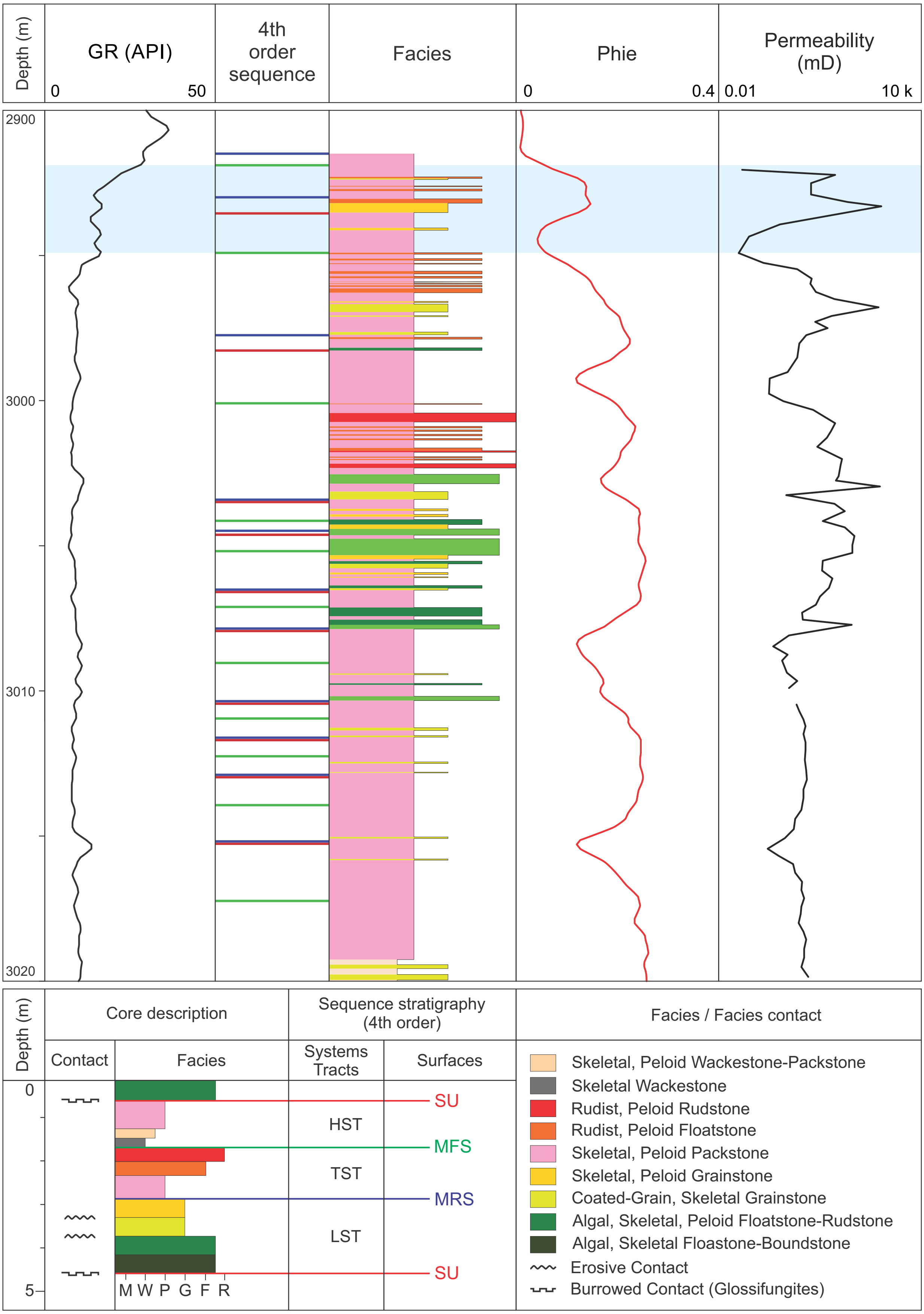

Phie: effective porosity.

Figure 34. The Upper Kharaib fourth-order reservoir zonation, Abu Dhabi, revealed the 2.1 m uppermost zone (highlighted in blue). The horizontal well drilled along that zone presents a threefold increase in the production rate compared to other wells in the field (modified from Torres *et al.* 2017).

Unexpected water breakthrough (i.e. water fingering, channeling, and coning) is a typical diagnostic feature that indicates the need for stratigraphic refinement. The oil/water contact rise may promote water coning in homogenous reservoirs (i.e. an uprising of water into the hydrocarbon interval due to pressure drawdown). However, reservoirs are much more heterogeneous than one would expect, and quite often, reservoir connectivity and heterogeneities are misrepresented or neglected in the 3D geological models. An example of water coning was observed in the Albian marine carbonate reservoirs from the Campos Basin in offshore Brazil (Bruhn *et al.* 2003). The reservoirs are part of elongated NE-trending shoals (< 1 km-wide, up to 2.5 km-long). The best reservoir facies consists of oncolite/oolite-rich grainstone, with porosity ranging between 20 and 34% and permeability exceeding 100 mD. They occur interbedded with lower-energy peloidal wackestone with shoaling-upward facies associations. The tight reservoir shows permeability around 5 mD. The uppermost intervals are the most productive of all, occurring preferably on faulted anticlines and rollover crests. The oil fields exhibit firm structural control, provided by faulting and bending. However, stratigraphic features — related to the lateral facies contact between grainstone/rudstone and packstone, wackestone, and mudstone also play an essential role in production (Bruhn *et al.* 2003). After production has started, the increase in water production encouraged the second seismic survey that revealed water coning consistent with the reservoir simulation model. The seismic survey demonstrated water uprising through permeable facies that control fluid flow through the reservoir (Fig. 35), thus indicating the need for stratigraphic refinement in order to allow oil production from the zones above and below the water-saturated zone.

A tilted oil/water contact can happen in particular situations that are subjected to effective bed-parallel hydrodynamic activity, such as in the Cretaceous Chalk Group and Paleocene sandstones in the Central North Sea (Dennis *et al.* 2000). However, tilted contacts often result from misinterpretation. In the Açu Formation in the Potiguar Basin, Brazil, an example from the Cretaceous meandering fluvial reservoir, the wells are only 93 m apart, and the contact shows a ten meter difference in elevation (Fig. 36, Melo *et al.* 2021). The high-resolution stratigraphic zonation demonstrated that there were two distinct contacts. Hence, different oil/water contacts in an oilfield help identify distinct zones and indicate the need for further stratigraphic refinement.

Moreover, the following diagnostic features may indicate the need for stratigraphic refinement, as observed in several producing oil fields:

- Geomechanical problems due to reservoir overpressure may lead to fracturing or fault reactivation, resulting in oil seeping on the surface or sea bottom. These problems usually happen due to the overestimation of the permeability or the lateral extent of the zone subjected to injection (e.g. Rutqvist *et al.* 2007, Amiri *et al.* 2019);
- Well drilling based on seismic anomalies not calibrated with the depositional model or the chronostratigraphic framework. Seismic anomalies do not always mean a reservoir has good porosity (e.g. Mojeddifar *et al.* 2015, Zampetti *et al.* 2017, Penna and Lupinacci 2021);
- Wells crossing unforeseen zones or unexpected fluids indicate we are unaware of the spatial distribution of reservoirs (Abraham *et al.* 2019);
- If the production curve does not match the observed historical data, one must review the facies distribution and

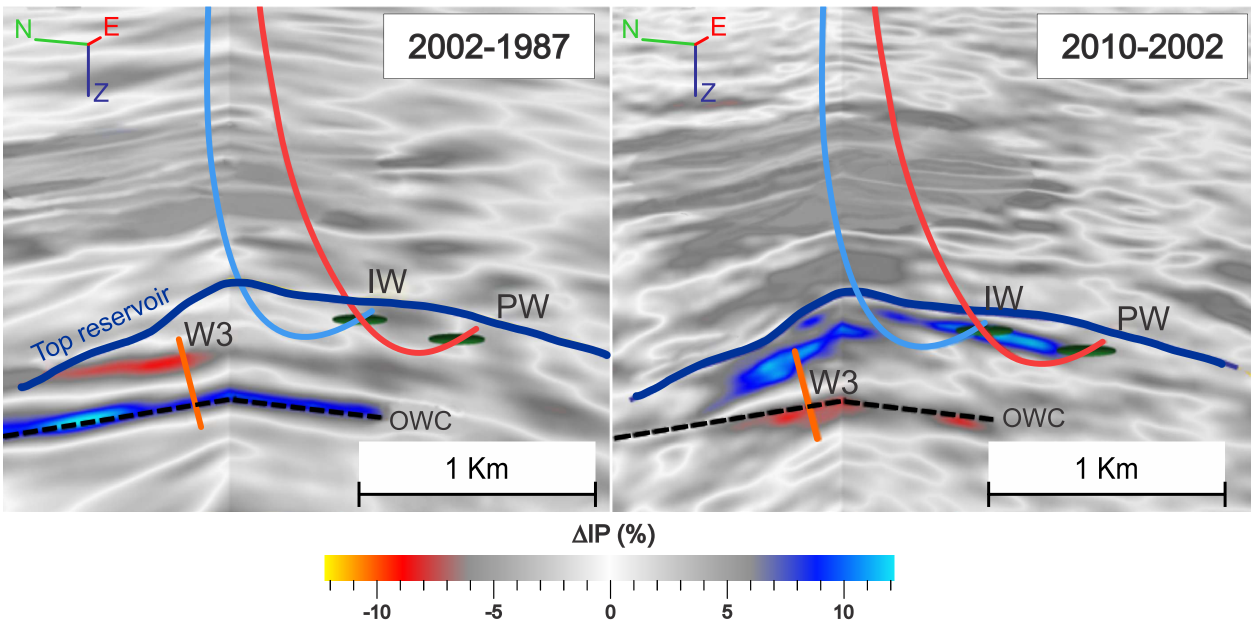

ΔIP: wave impedance variation; OWC: oil-water contact; IW: injection well; PW: production well.

Figure 35. Lithostratigraphic interpretation superimposed on a 4D seismic time-lapse in the Albian carbonate reservoir (offshore Brazil) shows ΔIP vertical sections resulting from the 4D joint inversion from 1987–2002 (left) 2002-2010 (right). The OWC at well W3 is observed from 1987 to 2002 as a flat positive IP anomaly. Note the water fingering affecting well W3, and water injected through well IW from 2002 to 2010, indicating the need for stratigraphic refinement in order to individualize zones within a previously assumed homogeneous reservoir (modified from Grochau *et al.* 2014).

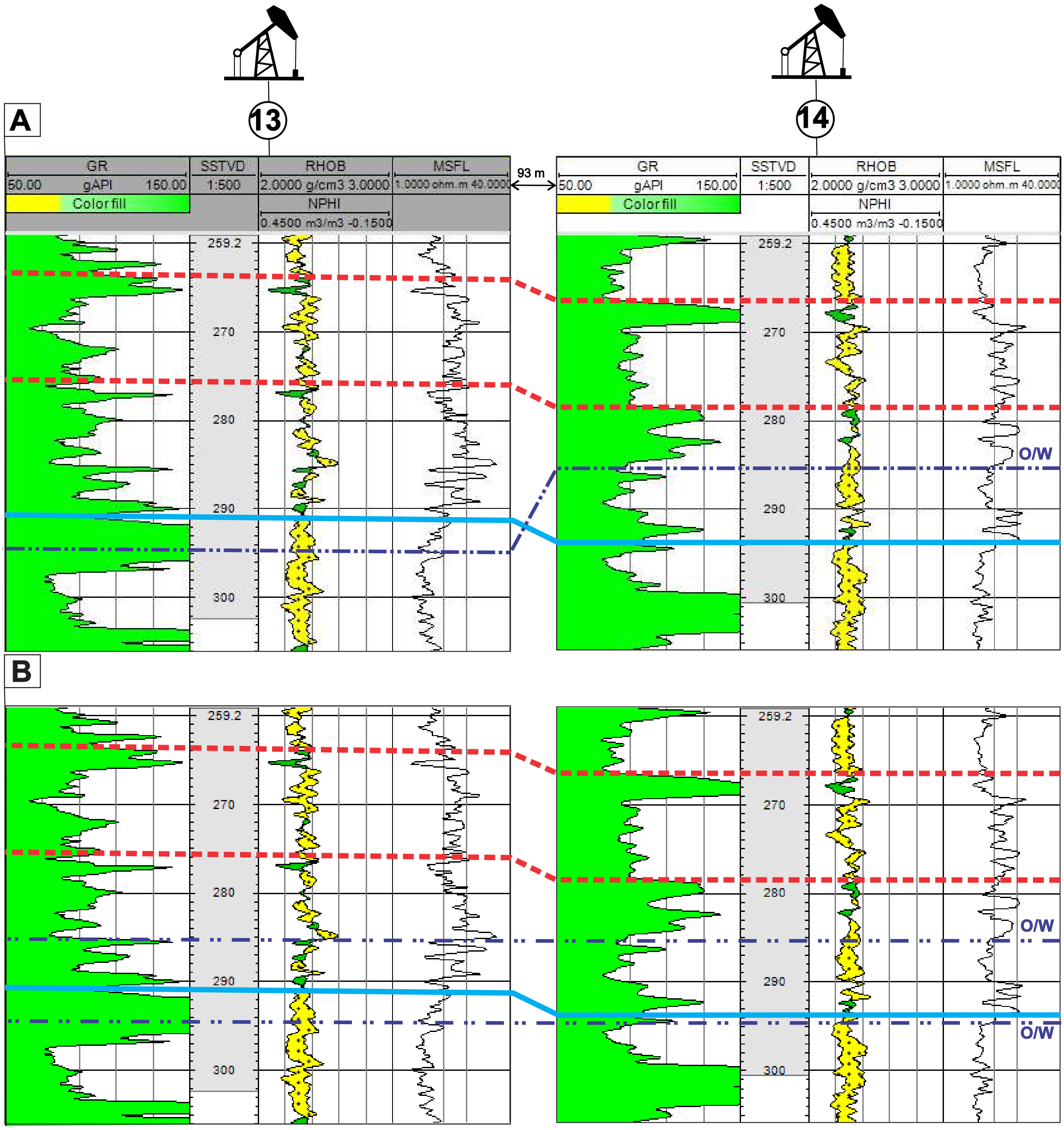

Figure 36. Structural section passing through wells 13 and 14. (A) Example of a tilted oil-water contact (dashed blue line). Note the ten meters difference in elevation between these wells spaced only 93 meters apart from each other. However, the high-resolution zonation showed that the "tilted contact" truncates the high-resolution zone boundary (blue line, MRS 2). (B) The high-resolution zonation demonstrated the presence of two distinct horizontal oil-water contacts instead of one tilted contact. (Cretaceous Açu Formation, Potiguar Basin, Brazil, Melo *et al.* 2018).

petrophysical properties within the zones. However, it is strongly recommended not to use artifacts to force the simulator to match (e.g. Avansi *et al.* 2016, Magalhães *et al.* 2020);

- Finally, the production forecast based on unadjusted geological and flow models inevitably leads to considerable deviation between prediction and observed production, resulting in financial loss (Singh and Srinivasan 2014, Razak and Jafarpour 2020).

FINAL REMARKS

Natural resources formed by or associated with sedimentary processes can be researched through sequence stratigraphy. This process-based stratigraphic analysis method unravels the evolution of sedimentation through time and space within sedimentary basins. Some examples include placer deposits associated with a subaerial unconformity or wave ravinement surface; bauxite with subaerial unconformity; coal seams and petroleum source rocks with maximum flooding surface; as well as phosphorites with a transgressive stacking pattern. In carbonate successions, the stratigraphic framework identifies epigenic karst intervals associated with a subaerial unconformity (super-k layers) and impermeable layers (zone boundaries) that overlie strata with dolomite cement and enhanced porosity and permeability. Therefore, the research, exploration, and production of any natural resource deposit whose formation is tied to sedimentary processes may be adequately addressed through sequence stratigraphy.

At the exploration scale, sequence stratigraphy focuses on evaluating the natural resource potential to make discoveries. At the production scale, high-resolution sequence stratigraphy (HRSS) highlights the spatial and temporal distribution of natural resource deposits and heterogeneities to optimize production. At both scales, the efficient application remains closely associated with the chronostratigraphic framework of the studied succession. In the petroleum industry, HRSS supports reservoir zonation and characterization, which are the essence of 3D geological and fluid flow models that guide reservoir management, production forecast and optimization, as well as increasing the ultimate recovery factor. Diagnostic features indicate the need for stratigraphic refinements, such as tilted or distinct fluids contacts and the difference between the simulated production and the observed historical data. In greenfields (i.e. new fields), HRSS identifies the best reservoirs for production, helping capital allocation, risk management and production costs. In brownfields (i.e. mature fields), it guides an increase in production that marks a new field rejuvenation phase. Besides, using 3D virtual outcrop models coupled with Ground Penetrating Radar has also significantly improved the stratigraphic analysis of outcropping successions as analogs for subsurface petroleum reservoirs.

ACKNOWLEDGEMENTS

This paper benefits from years of close cooperation among the authors and other colleagues involved with sequence stratigraphy. We thank Petroleum Experts Ltd for the Move Suite and Gustavo Barros for his drafting skills. We also thank Petrobras and its professionals who supported this work. Special thanks to Editor-in-Chief Claudio Riccomini for his careful attention to the manuscript and the anonymous reviewer for the constructive feedback.

ARTICLE INFORMATION

Manuscript ID: 20210014. Received on: 02/22/2021. Approved on: 08/03/2021.

A.M. wrote the first draft of the manuscript and prepared the figures; D.F. and G.P. revised and improved the manuscript; G.T. revised and improved the manuscript especially regarding carbonate; A.M. and P.A. provided data regarding application in the oil industry and revised the manuscript; F.G. provided data regarding virtual outcropping model and revised the manuscript; F.L. provided data regarding ground-penetrating radar and revised the manuscript.

Competing interests: The authors declare no competing interests.

REFERENCES

Abraham A.B., Evans A.B., Thompson B.E. 2019. Analysis of spatial distribution pattern of reservoir petrophysical properties for horizontal well performance evaluation-a case study of reservoir X. *The Open Petroleum Engineering Journal*, **12**(1):1-13. http://dx.doi.org/10.2174/1874834101912010001

Abram M.B., Bahiense I., Porto C.G., Brito R.S.C. (eds.). 2011. *Projeto Fosfato Brasil – Parte I*. Salvador: CPRM. Informe de Recursos Minerais, Série Insumos Minerais para a Agricultura, v. 13. Programa Geologia do Brasil. 526 p.

Abram M.B., Holz M. 2020. Early to Middle Devonian ironstone and phosphorites in the northwestern Gondwana Parnaíba Basin, Brazil: a record of an epeiric margin paleoceanographic changes. *Sedimentary Geology*, **402**:105646. https://doi.org/10.1016/j.sedgeo.2020.105646

Ainsworth R.B., Sanlung M., Theo S., Duivenvoorden C. 1999. Correlation techniques, perforation strategies, and recovery factors: An integrated 3-D reservoir modeling approach Sirkit Field, Thailand. *American Association of Petroleum Geologists Bulletin*, **83**:535-1551.

Aitken J.F., Howell J.A. (eds.). 1996. High-resolution sequence stratigraphy: innovations and applications. *Geological Society London Special Publications*, **104**:1-374. https://doi.org/10.1144/GSL.SP.1996.104.01.01

Allen G.P., Posamentier H.W. 1993. Sequence stratigraphy and facies model of an incised valley fill: the Gironde estuary, France. *Journal of Sedimentary Petrology*, **63**(3):378-391. https://doi.org/10.1306/D4267B09-2B26-11D7-8648000102C1865D

Allen J.R.L. 1983. Studies in fluviatile sedimentation: bars, bar complexes and sandstone sheets (low sinuosity braided streams) in the Brownstones (L. Devonian), Welsh Borders. *Sedimentary Geology*, **33**(4):237-293. https://doi.org/10.1016/0037-0738(83)90076-3

Amiri M., Lashkaripour G.R., Ghabezloo S., Moghaddas N.H., Tajareh M.H. 2019. Mechanical earth modeling and fault reactivation analysis for CO2-enhanced oil recovery in Gachsaran oil field, south-west of Iran. *Environmental Earth Sciences*, **78**:112. https://doi.org/10.1007/s12665-019-8062-1

Annan A.P. 2009. Ground Penetrating Radar (GPR) Principles. *In*: Jol H. (ed.). *Ground penetrating radar theory and applications*. Amsterdam: Elsevier. p. 4-38.

Asmus H.E., Porto R. 1980. Diferenças nos estágios iniciais da evolução da margem continental brasileira: possíveis causas e implicações. *In*: Congresso Brasileiro de Geologia, 31., 1980, Camboriú. *Annals...*, p. 225-239.

Avansi G.D., Maschio C., Schiozer D.J. 2016. Simultaneous history-matching approach by use of reservoir-characterization and reservoir-simulation studies. *SPE Reservoir Evaluation & Engineering*, **19**(4):694-712. https://doi.org/10.2118/179740-PA

Bhattacharya J.P. 1993. The expression and interpretation of marine flooding surfaces and erosional surfaces in core: examples from the Upper Cretaceous Dunvegan Formation in the Alberta foreland basin. *In*: Summerhayes C.P., Posamentier H.W. (eds.). *Sequence stratigraphy and facies associations*. International Association of Sedimentologists Special Publication, **18**:125-160.

Bhattacharya J.P., Walker R.G. 1991. Allostratigraphic subdivision of the Upper Cretaceous Dunvegan, Shaftesbury, and Kaskapau Formations in the subsurface of northwestern Alberta. *Bulletin of Canadian Petroleum Geology*, **39**(2):145-164. https://doi.org/10.35767/gscpgbull.39.2.145

Bento Freire E. 2012. *Caracterização estratigráfica em alta resolução das sequências carbonáticas de origem microbial do intervalo paleocênico da Formação Yacoraite (Sequência Balbuena IV) na região de Salta – Argentina*. MSc thesis, Universidade Federal do Rio de Janeiro, Rio de Janeiro, 224 p.

Bermejo L., Ortega A.I., Parés J.M., Campaña I., Castro J.M.B., Carbonell E., Conyers L.B. 2020. Karst features interpretation using ground-penetrating radar: A case study from the Sierra de Atapuerca, Spain. *Geomorphology*, **367**:107311. https://doi.org/10.1016/j.geomorph.2020.107311

Bird J.M., Dewey J.F. 1970. Lithosphere plate-continental margin tectonics and the evolution of the Appalachian orogeny. *Bulletin of the Geological Society of America*, **81**(4):1031-1060. https://doi.org/10.1130/0016-7606(1970)81[1031:LPMTAT]2.0.CO;2

Bögli A. 1980. *Karst hydrology and physical speleology*. Berlin: Springer-Verlag, 284 p.

Bohacs K.M., Carroll A.R., Jeal J.E., Mankiewicz P.J. 2000. Lake-Basin Type, source potential, and hydrocarbon character: An integrated sequence-stratigraphic-geochemical framework. *In*: Gierlowski-Kordesch E.H., Kelts K.R. (eds.). *Lake basins through space and time*. American Association of Petroleum Geologists Studies in Geology, **46**:3-34.

Bohacs K.M., Suter J. 1997. Sequence stratigraphic distribution of coaly rocks: fundamental controls and paralic examples. *American Association of Petroleum Geologists Bulletin*, **81**(10):1612-1639.

Bristow C.S., Jol H.M. 2003. *Ground penetrating radar in sediments*. London: Geological Society, Special Publications, 211 p.

Brookfield M.E. 1977. The origin of boundaries in ancient aeolian sandstones. *Sedimentology*, **24**(3):303-332. https://doi.org/10.1111/j.1365-3091.1977.tb00126.x

Brown L.F. Jr., Fisher W.L. 1977. Seismic–stratigraphic interpretation of depositional systems: examples from Brazilian rift and pull-apart basins. *In*: Payton (ed.). *Seismic stratigraphy applications to hydrocarbon exploration*. American Association of Petroleum Geologists, Memoir, **26**:213-248.

Bruhn C.H.L., Gomes J.A.T., Lucchese Jr. C., Johann P.R.S. 2003. Campos Basin: reservoir characterization and Management – Historical Overview and future challenges. *In*: Offshore Technology Conference, Houston, OTC 15220, 14 p.

Bruhn C.H.L., Pinto A.C.C., Johann P.R.S., Branco C.C.M., Salomão M.C., Freire E.B. 2017. Campos and Santos Basins: 40 years of reservoir characterization and management of shallow to ultra deep water, post and pre-salt reservoirs historical overview and future challenges. *In*: Offshore Technology Conference, Rio de Janeiro, OTC 28159 MS.

Bruun P. 1962. Sea-level rise as a cause of shore erosion. *Journal of the Waterways and Harbors Division*, **88**(1):117-130. https://doi.org/10.1061/JWHEAU.0000252

Buckley S.J., Ringdal K., Naumann N., Dolva B., Kurz T.H., Howell J.A., Dewez T.J.B. 2019. LIME: Software for 3-D visualization, interpretation, and communication of virtual geoscience models. *Geosphere*,**15**(1):222-235. https://doi.org/10.1130/GES02002.1

Bunevich R.B., Borghi L., Raja Gabaglia G.P., Terra G.J.S., Bento Freire E., Lykawka R., Fragoso D.G.C. 2017. Microbialitos da Sequência Balbuena IV (Daniano), Bacia de Salta, Argentina: caracterização de intrabioarquiteturas e de microciclos. Universidade Federal do Rio Grande do Sul, Brasil. *Pesquisas em Geociências*, **44**(2):177-202. https://doi.org/10.22456/1807-9806.78270

Burnham B.S., Hodgetts D. 2019. Quantifying spatial and architectural relationships from fluvial outcrops. *Geosphere*, **15**(1):236-253. https://doi.org/10.1130/GES01574.1

Castelltort S., Van Den Driessche J. 2003. How plausible are high-frequency sediment supply-driven cycles in the stratigraphic record? *Sedimentary Geology*, **157**(1-2):3-13. https://doi.org/10.1016/S0037-0738(03)00066-6

Catuneanu O. 2006. *Principle of sequence stratigraphy*. Amsterdam: Elsevier, 375 p.

Catuneanu O. 2017. Sequence stratigraphy: guidelines for a standard methodology. *In*: Montenari, M. (ed.). *Stratigraphy & Timescales*. United Kingdom: Academic Press, **2**:1-57.

Catuneanu O. 2019. Model-independent sequence stratigraphy. *Earth-Science Reviews*, **188**:312-388. https://doi.org/10.1016/j.earscirev.2018.09.017

Catuneanu O., Biddulph M.N. 2001. Sequence stratigraphy of the Vaal Reef facies associations in the Witwatersrand foredeep, South Africa. *Sedimentary Geology*, **141-142**:113-130. https://doi.org/10.1016/S0037-0738(01)00071-9

Catuneanu O., Galloway W.E., Kendall C.G.St.C., Miall A.D., Posamentier H.W., Strasser A. 2011. Sequence stratigraphy: methodology and nomenclature. *Newsletters on Stratigraphy*, **44**(3):173-245. https://doi.org/10.1127/0078-0421/2011/0011

Choquette P.W., Pray L.C. 1970. Geological nomenclature and classification of porosity in sedimentary carbonates. *American Association of Petroleum Geologists Bulletin*, **54**(2):207-250. https://doi.org/10.1306/5D25C98B-16C1-11D7-8645000102C1865D

Correa C.R.A., Lykawka R., Lourenço A.T.A., Silva A.P., Reis F.N., Leviski T.F. 2013. 3D geological modelling of a karstified carbonate reservoir support on seismic attributes and dynamic well data, Campos Basin, Brazil. *In*: International Conference & Exhibition, 2013. American Association of Petroleum Geologists, Article #90166.

Davies G.R., Smith Jr. L.B. 2006. Structurally controlled hydrothermal dolomite reservoir facies: an overview. *American Association of Petroleum Geologists Bulletin*, **90**(11):1641-1690. https://doi.org/10.1306/05220605164

De Gasperi A., Catuneanu O. 2014. Sequence stratigraphy of the Eocene turbidite reservoirs in Albacora field, Campos Basin, offshore Brazil. *American Association of Petroleum Geologists Bulletin*, **98**(2):279-313. https://doi.org/10.1306/07031312117

Della Fávera J.C., Chaves H.A.F., Medeiros M.A.M., Villares J.T.L., Souza S.F.M., Oliveira S.S., Martins M.V.A. 2019. Stratigraphic analysis of the Aratu Stage (Lower Cretaceous), Recôncavo Basin (Brazil), with hydrocarbon reservoir rocks. *Journal of Sedimentary Environments*, **4**(2):199-219. https://doi.org/10.12957/jse.2019.43784

Dennis H., Baillie J., Holt T., Wessel-Berg D. 2000. Hydrodynamic activity and tilted oil-sater contacts in the North Sea. *Norwegian Petroleum Society Special Publications*, **9**:171-185. https://doi.org/10.1016/S0928-8937(00)80016-8

Dewey J.F., Bird J.M. 1970. Mountain belts and the new global tectonics. *Journal of Geophysical Research*, **75**(14):2625-2647. https://doi.org/10.1029/JB075i014p02625

Dickinson W.R. 1971. Plate tectonic models of geosynclines. *Earth and Planetary Science Letters*, **10**(2):165-174. https://doi.org/10.1016/0012-821X(71)90002-1

Dickson J.A.D. 2004. Echinoderm skeletal preservation: calcite–aragonite seas and the Mg/Ca ratio of Phanerozoic oceans. *Journal of Sedimentary Research*, **74**(3):355-365. https://doi.org/10.1306/112203740355

Dominguez J.M.L., Wanless H.R. 1991. Facies architecture of a falling sea-level stranplain, Doce River coast, Brazil. *In*: Swift D.J.P., Oertel G.F., Tilman R.W., Thorne J.A. (eds.). Shelf sand and sandstone bodies: geometry, facies and sequence stratigraphy. *International Association of Sedimentologists Special Publication*, **14**:259-281. https://doi.org/10.1002/9781444303933.ch7

Dougherty A.J., Choi J., Turney C.S.M., Dosseto A. 2019. Technical note: Optimizing the utility of combined GPR, OSL, and Lidar (GOaL) to extract paleoenvironmental records and decipher shoreline Evolution. *Climate of the Past*, **15**(1):389-404. https://doi.org/10.5194/cp-15-389-2019

Eichenseer H.T., Walgenwitz F.R., Biondi P.J. 1999. Stratigraphic control on facies and diagenesis of dolomitized sequences (Pinda Group, Albian, offshore Angola). *American Association of Petroleum Geologists Bulletin*, **83**(11):1729-1758. https://doi.org/10.1306/E4FD4251-1732-11D7-8645000102C1865D

Einsele G., Ricken W., Seilacher A. (eds.). 1991. *Cycles and events in stratigraphy*. Berlin: Springer-Verlag, 955 p.

Embry A.F. 1995. Sequence boundaries and sequence hierarchies: problems and proposals. *Norwegian Petroleum Society Special Publications*, **5**:1-11. https://doi.org/10.1016/S0928-8937(06)80059-7

Embry A.F., Johannessen E.P. 1992. T-R sequence stratigraphy, facies analysis and reservoir distribution in the uppermost Triassic-Lower Jurassic succession, western Sverdrup Basin, Artic Canada. *In*: Vorren T.O., Bergsager E., Dahl-Stamnes O.A., Holter E., Johansen B., Lie E., Lund T.B. (eds.). *Artic geology and petroleum potential*. Norwegian Petroleum Society Special Publication, **2**:121-146.

Feazel C.T., Schatzinger R.A. 1985. Prevention of carbonate cementation in petroleum reservoirs. *In*: Schneidermann N., Harris P.M. (eds.). *Carbonate cements*. Society of Economic Paleontologists and Mineralogists Special Publication, **36**:97-106.

Fragoso D.G.C., Raja Gabaglia G.P., Magalhães A.J.C., Scherer C.M.S. 2021. Cyclicity and hierarchy in sequence stratigraphy: an integrated approach. *Brazilian Journal of Geology*, **51**(2):e20200106. https://doi.org/10.1590/2317-4889202120200106

Frazier D.E. 1974. Depositional episodes: their relationship to the Quaternay stratigraphic framework in the northwestern portion of the Gulf Basin. University of Texas at Austin, Bureau of Economic Geology, *Geological Circular*, **74**(1), 28 p. https://doi.org/10.23867/gc7401D

Galloway W.E. 1989. Genetic stratigraphic sequences in basin analysis, I. Architecture and genesis of flooding-surface bounded depositional units. *American Association of Petroleum Geologists Bulletin*, **73**(2):125-142. https://doi.org/10.1306/703C9AF5-1707-11D7-8645000102C1865D

Gilbert G.K., Murphy E.C. 1914. The transportation of debris by running water. *U.S. Geological Survey Professional Paper*, 86, 221 p. https://doi.org/10.3133/pp86

Grabau A.W. 1906. Types of sedimentary overlap. *Geological Society American Bulletin*, **17**(1):567-636. https://doi.org/10.1130/GSAB-17-567

Grochau M.H., Benac P.M., Alvim L.M., Sansonowski R.C., Pires P.R.M., Villaudy F. 2014. Brazilian carbonate reservoir: a successful seismic time-lapse monitoring study. *The Leading Edge*, **33**(2):164-170. https://doi.org/10.1190/tle33020164.1

Handford C.R., Loucks R.G. 1991. Unique signature of carbonate strata and the development of depositional sequence and systems tract models for ramps, rimmed shelves, and detached platforms (Abstract). *American Association of Petroleum Geologists Bulletin*, **75**(3):588-589.

Handford C.R., Loucks R.G. 1993. Carbonate depositional sequences and systems Tracts – Responses of carbonate platforms to relative sea-level changes. *In*: Loucks R.G., Sarg J.F. (eds). *Carbonate sequence stratigraphy*. Recent Developments and Applications. American Association of Petroleum Geologists, Memoir, **57**:3-42.

Helland-Hansen W., Martinsen O.J. 1996. Shoreline trajectories and sequences: description of variable depositional-dip scenarios. *Journal of Sedimentary Research*, **66**(4):670-688. https://doi.org/10.1306/D42683DD-2B26-11D7-8648000102C1865D

Hill C.A. 1995. H_2S-related porosity and sulfuric acid oil-field karst. *In*: Budd D.A., Saller A.H., Harris P.M. (eds.). *Unconformities and Porosity in Carbonate Strata*. American Association of Petroleum Geologists Memoir, **63**:301-306.

Hodgetts D. 2013. Laser scanning and digital outcrop geology in the petroleum industry: a review. *Marine and Petroleum Geology*, **46**:335-354. https://doi.org/10.1016/j.marpetgeo.2013.02.014

Holbrook J., Miall A.D. 2020. Time in the rock: a field guide to interpreting past events and processes from siliclastic stratigraphy. *Earth Science Reviews*, **203**:103121. https://doi.org/10.1016/j.earscirev.2020.103121

Holz M., Kalkreuth W., Banerjee I. 2002. Sequence stratigraphy of paralic coal-bearing strata: an overview. *International Journal of Coal Geology*, **48**(3-4):147-179. https://doi.org/10.1016/S0166-5162(01)00056-8

Howell J.A., Martinius A.W., Good T.R. 2014. The application of outcrop analogues in geolocial modelling: a review, present status and future outlook. *In*: Martinius A.W., Howell J.A., Good T.R. (eds). *Sediment-body geometry and heterogeneity:* analogue studies for modelling the subsurface. London: Geological Society of London, p. 1-25.

Hunt D., Tucker M.E. 1992. Stranded parasequences and the forced regressive wedge systems tract: deposition during base-level fall. *Sedimentary Geology*, **81**(1-2):1-9. https://doi.org/10.1016/0037-0738(92)90052-S

Jervey M.T. 1988. Quantitative geological modeling of siliciclastic rock sequences and their seismic expression. *In*: Wilgus C.K., Hastings B.S., Kendall C.G.St.C., Posamentier H.W., Ross C.A., Van Wagoner J.C. (eds.). *Sea level changes:* an integrated approach. Society of Economic Paleontologists and Mineralogists Special Publication, **42**:47-69.

Jol H.M. 1995. Ground penetrating radar antennae frequencies and transmitter powers compared for penetration depth, resolution and reflection continuity. *Geophysical Prospecting*, **43**(5):693-709. https://doi.org/10.1111/j.1365-2478.1995.tb00275.x

Jones B. 2010. Warm-water neriic carbonates. *In*: James N.P., Dalrymple R.W. (eds.). *Facies Models 4*. Geologial Association of Canada, **6**:341-369.

Kechiched R., Laouar R., Bruguier O., Kocsis L., Salmi-Laouar S., Bosch D., Ameur-Zaimeche O., Fougou A., Larit H. 2020. Comprehensive REE + Y and sensitive redox trace elements of Algerian phosphorites (Tébessa, eastern Algeria): A geochemical study and depositional environments tracking. *Journal of Geochemical Exploration*, **208**:106396. https://doi.org/10.1016/j.gexplo.2019.106396

Klimchouk A. 2017. Types and settings of hypogene karst. *In*: Klimchouck A., Palmer A.N., De Waele J., Auler A.S., Audra P. (eds.). *Hypogene karst regions and caves of the world:* cave and kart systems of the world. Berlin: Springer, 911 p.

Leandro C.G., Barbosa G.E., Caron F., Jesus F.A.N. 2019. GPR trace analysis for coastal depositional environments of southern Brazil. *Journal of Applied Geophysics*, **162**:1-12. https://doi.org/10.1016/j.jappgeo.2019.01.002

Lear C.H., Anand P., Blenkinsop T., Foster G.L., Gagen M., Hoogakker B., Larter R.D., Lunt D.J., McCave I.N., McClymont E., Pancost R.D., Rickaby R.E.M., Schultz D.M., Summerhayes C., Williams C.J.R., Zalasiewicz J. 2020. Geological Society of London Scientific Statement: what the geological record tells us about our present and future climate. *Journal of the Geological Society,* **178**(1):2020-239. https://doi.org/10.1144/jgs2020-239

Loutit T.S., Handenbol J., Vail P.R., Baum G.R. 1988. Condensed sections: the key to age-dating and correlation of continental margin sequences. *In*: Wilgus C.K., Hastings B.S., Kendall C.G.St.C., Posamentier H.W., Ross C.A., Van Wagoner J.C. (eds.). *Sea level changes* – an integrated approach. Society of Economic Paleontologists and Mineralogists Special Publication, **42**:183-213.

Magalhães A.J.C., Lima-Filho F.P., Guadagnin F., Silva V.A., Teixeira W.L.E., Souza A.M., Raja Gabaglia G.P., Catuneanu O. 2017. Ground penetrating radar for facies architecture and high-resolution stratigraphy: Examples from the Mesoproterozoic in the Chapada Diamantina Basin, Brazil. *Marine and Petroleum Geology*, **86**:1191-1206. https://doi.org/10.1016/j.marpetgeo.2017.07.027

Magalhães A.J.C., Raja Gabaglia G.P., Fragoso D.G.C., Bento Freire E., Lykawka R., Arregui C.D., Silveira M.M.L., Carpio K.M.T., De Gasperi A., Pedrinha S., Artagão V.M., Terra G.J.S., Bunevich R.B., Roemers-Oliveira E., Gomes J.P., Hernández J.I., Hernández R.M., Bruhn C.H.L. 2020. High-resolution sequence stratigraphy applied to reservoir zonation and characterisation, and its impact on production performance - shallow marine, fluvial downstream, and lacustrine carbonate settings. *Earth-Science Reviews*, 103325. https://doi.org/10.1016/j.earscirev.2020.103325

Magalhães A.J.C., Raja Gabaglia G.P., Scherer C.M.S., Bállico M.B., Guadagnin F., Bento Freire E., Silva Born L.R., Catuneanu O. 2016. Sequence hierarchy in a Mesoproterozoic interior sag basin: from basin fill to reservoir scale, the Tombador Formation, Chapada Diamantina Basin, Brazil. *Basin Research*, **28**(3):393-432. https://doi.org/10.1111/bre.12117

Magalhães A.J.C., Scherer C.M.S., Raja Gabaglia G.P., Bállico M.B., Catuneanu O. 2014. Unincised fluvial and tide-dominated estuarine systems from the Mesoproterozoic Lower Tombador Formation, Chapada Diamantina basin, Brazil. *Journal of South American Earth Sciences*, **56**:68-90. https://doi.org/10.1016/j.jsames.2014.07.010

Magalhães A.J.C., Scherer C.M.S., Raja Gabaglia G.P., Catuneanu O. 2015. Mesoproterozoic delta systems of the Açuruá Formation, Chapada Diamantina, Brazil. *Precambrian Research*, **257**:1-21. https://doi.org/10.1016/j.precamres.2014.11.016

Magalhães A.J.C., Terra G.J.S., Guadagnin F., Fragoso D.G.C., Menegazzo M.C., Pimental N.L.A., Kumaira S., Fauth G., Santos A., Watkins D.A., Bruno M.D.R., Ceolin D., Baecker-Fauth S., Raja Gabaglia G.P., Teixeira W.L.E., Lima-Filho F.P. 2021. Stratigraphic record of cyclic low- and hig-energy sedimentation in a muddy, mixed siliciclastic-carbonate shelf, Middle Jurassic of the Central Lusitanian Basin. In press.

Marques Jr. A., Horota R.K., Souza E.M., Kupssinskü L., Rossa P., Aires A.S., Bachi L., Veronez M.R., Gonzaga Jr. L., Cazarin C.L. 2020. Virtual and digital outcrops in the petroleum industry: A systematic review. *Earth Science Reviews*, **208**:103260. https://doi.org/10.1016/j.earscirev.2020.103260

Mazzullo S.J., Harris P.M. 1992. Mesogenetic dissolution: its role in porosity development in carbonate reservoirs. *American Association of Petroleum Geologists Bulletin*, **76**(5):607-620. https://doi.org/10.1306/BDFF8880-1718-11D7-8645000102C1865D

McKee E.D., Weir G.W. 1953. Terminology for stratification and cross-stratification in sedimentary rocks. *Bulletin of the Geological Society of America*, **64**(4):381-390. https://doi.org/10.1130/0016-7606(1953)64[381:TFSACI]2.0.CO;2

Medina P.Z., Limarino C., Bonono N., Bernárdez S.S., Ossella A. 2020. Using Ground Penetrating Radar and attribute analysis for identifying depositional units in a fluvial-aeolian interaction environment: The Guandacol Valley, northwest Argentina. *Journal of South American Earth Sciences*, **98**:102467. https://doi.org/10.1016/j.jsames.2019.102467

Melo A.H., Andrade P.R.O., Magalhães A.J.C., Fragoso D.G.C., Lima-Filho F.P. 2020. Stratigraphic evolution from the early Albian to late Campanian of the Potiguar Basin, Northeast Brazil: An approach in seismic scale. *Basin Research*, **32**(5):1054-1080. https://doi.org/10.1111/bre.12414

Melo A.H., Magalhães A.J.C., Menegazzo M.C., Fragoso D.G.C., Florencio C.P., Lima-Filho F.P. 2021. High-resolution sequence stratigraphy applied for the improvement of hydrocarbon production and reserves: A case study in Cretaceous fluvial deposits of the Potiguar basin, northeast Brazil. *Marine and Petroleum Geology*, **130**, 105124. https://doi.org/10.1016/j.marpetgeo.2021.105124

Miall A.D. 1985. Architectural-elements analysis: a new method of facies analysis applied to fluvial deposits. *Earth-Science Reviews*, **22**(4):261-308. https://doi.org/10.1016/0012-8252(85)90001-7

Mial A.D. 1995. Whither stratigraphy? *Sedimentary Geology*, **100**(1-4):5-20. https://doi.org/10.1016/0037-0738(95)00100-X

Miall A.D., Arush M. 2001. Cryptic sequence boundaries in braided fluvial successions: *Sedimentology*, **48**(5):971-985. https://doi.org/10.1046/j.1365-3091.2001.00404.x

Middleton G.V. (ed.). 1965. Primary sedimentary structures and their hydrodynamic interpretation. *Society for Sedimentary Geology Special Publication*, **12**, 265 p. https://doi.org/10.2110/pec.65.08

Mitchum R.M. 1977. Seismic stratigraphy and global changes of sea level, Part 1: Glossary of terms used in seismic stratigraphy. *In*: Payton C.E. (ed.). *Seismic Stratigraphy – Applications to hydrocarbon exploration*. American Association of Petroleum Geologists, Memoir, **26**:205-212.

Mitchum Jr. R.M., Vail P.R. 1977. Seismic stratigraphy and global changes or sea-level, part 7: stratigraphic interpretation of seismic reflection patterns in depositional sequences. *In*: Payton C.E. (ed.). *Seismic Stratigraphy – Applications to hydrocarbon exploration*. American Association of Petroleum Geologists, Memoir, **26**:135-144.

Mojeddifar S., Kamali G., Ranjbar H. 2015. Porosity prediction from seismic inversion of a similarity attribute based on a pseudo-forward equation (PFE): a case study from the North Sea Basin, Netherlands. *Petroleum Science*, **12**:428-442. https://doi.org/10.1007/s12182-015-0043-8

Moore C.H. 2010. *Carbonate reservoirs:* porosity evolution and diagenesis in a sequence stratigraphy framework, developments in sedimentology 55. Amsterdam, Elsevier, 444 p.

Mossop G.D. 1980. Geology of the athabasca oil sands. *Science*, **207**(4427):145-152. https://doi.org/10.1126/science.207.4427.145

Neal J., Abreu V. 2009. Sequence stratigraphy hierarchy and the accommodation succession method, *Geology*, **37**(9):779-782. https://doi.org/10.1130/G25722A.1

Palmer A.N. 1991. Origin and morphology of limestone caves. *Geological Society of America Bulletin*, **103**(1):1-21. https://doi.org/10.1130/0016-7606(1991)103%3C0001:OAMOLC%3E2.3.CO;2

Payton C.E. (ed.). 1977. *Seismic stratigraphy:* applications to hydrocarbon exploration. American Association of Petroleum Geologists, Memoir, **26**, 516 p.

Pedrinha S. 2014. *Análise estratigráfica em depósitos lacustres Maastrichianos da Formação Yacoraite (Bacia de Salta – Argentina): definição e rastreabilidade de sequências de alta resolução*. MSc thesis, Universidade Estadual Paulista "Júlio de Mesquita Filho", Brasil, 148 p.

Penna R., Lupinacci W.M. 2021. 3D modelling of flow units and petrophysical properties in Brazilian presalt carbonate. *Marine and Petroleum Geology*, **124**:104829. https://doi.org/10.1016/j.marpetgeo.2020.104829

Pistis M., Loi A., Dabard M.P. 2016. Influence of relative sea-level variations on the genesis of paleoplacers, the examples of Sarrabus (Sardinia, Italy) and the Armorican Massif (western France). *Comptes Rendus Geoscience*, **348**(2):150-157. https://doi.org/10.1016/j.crte.2015.09.006

Plint A.G. 1988. Sharp-based shoreface sequences and "offshore bars" in the Cardium Formation of Alberta; their relationship to relative changes in sea level. *In*: Wilgus C.K., Hastings B.S., Kendall C.G.St.C., Posamentier H.W., Ross C.A., Van Wagoner J.C. (eds.). *Sea level changes:* an integrated approach. Society of Economic Paleontologists and Mineralogists Special Publication, **42**:357-370.

Pomar L. 1993. High-resolution sequence stratigraphy in prograding Miocene carbonates: application to seismic interpretation. *In*: Loucks R.G., Sarg J.F. (eds.). *Carbonate sequence stratigraphy*. American Association of Petroleum Geologists, Memoir, **57**:389-407.

Pomar L. 2020. Carbonate Systems. *In*: Scarselli N., Adam J., Chiarella D., Roberts D.G., Bally A.W. (eds.). *Regional geology and tectonics:* principles of geologic analysis. 2ª ed. Amsterdam: Elsevier, v. 1, 744 p.

Pomar L., Haq B.U. 2016. Decoding depositional sequences in carbonate systems: Concepts vs experience. *Global and Planetary Change*, **146**:190-225. https://doi.org/10.1016/j.gloplacha.2016.10.001

Posamentier H.W. 2001. Lowstand alluvial bypass systems: incised vs. unincised. *American Association of Petroleum Geologists Bulletin*, **85**(10):1771-1793. http://dx.doi.org/10.1306/8626D06D-173B-11D7-8645000102C1865D

Posamentier H.W., Allen G. 1999. Siliciclastic sequence stratigraphy – concepts and applications. *In*: Posamentier H.W., Allen G. (eds.). *Concepts in Sedimentology and Paleontology*. Society of Economic Paleontologists and Mineralogists, 7, 210 p.

Posamentier H.W., Jervey M.T., Vail P.R. 1988. Eustatic controls on clastic deposition I – conceptual framework. *In*: Wilgus C.K., Hastings B.S., Kendall C.G.St.C., Posamentier H.W., Ross C.A., Van Wagoner J.C. (eds.). *Sea level changes:* an integrated approach. Society of Economic Paleontologists and Mineralogists Special Publication, **42**:110-124.

Razak S.M., Jafarpour B. 2020. Rapid Production Forecasting with Geologically-Informed Auto-Regressive Models: Application to Volve Benchmark Model. *In*: SPE Annual Technical Conference and Exhibition, 1-7. https://doi.org/10.2118/201356-MS

Reijenstein H.M., Posamentier H.W., Bhattacharya J.P. 2011. Seismic geomorphology and high-resolution seismic stratigraphy of inner-shelf, fluvial, estuarine, deltaic, and marine sequences, Gulf of Thailand. *American Association of Petroleum Geologists Bulletin*, **95**(11):1959-1990. http://dx.doi.org/10.1306/03151110134

Renaut R.W., Gierlowski-Kordesch E.H. 2010. Lakes. *In*: James N.P., Dalrymple R.W. (Eds.). *Facies models 4*. Geological Association of Canada Geotext, **6**:541-575.

Roemers-Oliveira E., Fernandes L.A., Bento Freire E., Simões L.S.A. 2015. Microbial filaments in stromatolites and laminites of Balbuena III Sequence (Maastrichtian/Danian) of Yacoraite Formation in Metán-Alemania Sub-basin, Salta region, Argentina, and its paleoenvironmental significance. *Brazilian Journal of Geology*, **45**(3):399-413. https://doi.org/10.1590/2317-488920150030255

Romans B.W., Castelltort S., Covault J.A., Fildani A., Walsh J. 2016. Environmental signal propagation in sedimentary systems across timescales. *Earth-Science Reviews*, **153**:7-29. https://doi.org/10.1016/j.earscirev.2015.07.012

Rutqvist J., Birkholzer J.T., Cappa F., Tsang C.F. 2007. Estimating maximum sustainable injection pressure during geological sequestration of CO2 using coupled fluid flow and geomechanical fault-slip analysis. *Energy Conversion and Management*, **48**(6):1798-1807. https://doi.org/10.1016/j.enconman.2007.01.021

Selley R.C. 1970. *Ancient sedimentary environments and their subsurface diagnosis*. 4ª ed. New York: Routledge, 237 p.

Shanley K.W., McCabe P.J. 1994. Perspectives on the sequence stratigraphy of continental strata. *American Association of Petroleum Geologists Bulletin*, **78**(4):544-568.

Simons D.B., Richardson E.W., Albertson M.L. 1961. Flume studies using medium sand (0.45 mm). *United States Geological Survey Water-Supply Paper 1498-A*, 76 p. https://doi.org/10.3133/wsp1498A

Singh H., Srinivasan S. 2014. Assessing economic implications of complexity in geological modeling and simulation. In: SPE Hydrocarbon Economics and Evaluation Symposium, Houston. *Annals…*, p. 1-18. https://doi.org/10.2118/169825-MS

Souza P.E., Kroon A., Nielsen L. 2018. Beach-ridge architecture constrained by beach topography and ground-penetrating radar, Itilleq (Laksebugt), south-west Disko, Greenland - implications for sea-level reconstructions. *Bulletin of the Geological Society of Denmark*, **66**:167-179. http://dx.doi.org/10.37570/bgsd-2018-66-08

Swift D.J.P. 1975. Barrier-island genesis: evidence from the central Atlantic shelf, eastern USA. *Sedimentary Geology*, **14**(1):1-43. https://doi.org/10.1016/0037-0738(75)90015-9

Terra G.J.S. 1990. *Facies, modelo deposicional e diagênese da sequência carbonática Albo-Cenomaniana (Formação Ponta do Mel) da Bacia Potiguar*. MSc thesis, Universidade Federal do Rio de Janeiro, Rio de Janeiro, 154 p.

Thompson C., McMechan G., Szerbiak R., Gaynor N. 1995. Three-dimensional GPR imaging of complex stratigraphy within the Ferron sandstone, Castle Valley, Utah. *In*: Symposium on the Application of Geophysics to Engineering and Environmental Problems, 1995. *Proceedings…*, p. 435-443.

Tibana P., Terra G.J.S. 1981. Sequências carbonáticas do Cretáceo da Bacia Potiguar. *Boletim Técnico da Petrobras*, **24**(3):174-183.

Torres K.M., Pozo E.G. Robladillo J.F.C., Ramírez E.J.B. 2012. Estratigrafía secuencial de alta resolución aplicada a reservorios maduros: propuesta de correlación de secuencias genéticas de 5to orden para la definición de unidades de flujo – Fm. Echinocyamus, Eoceno-Ypresiano, Lote X, Cuenca Talara, Perú. *In*: XVI Peruvian Geological Congress and SEG Conference, 16., 2012, Lima. Annals...

Torres K.M., Ugonoh M.S., Al Hashmi N.F. 2017. High-resolution sequence stratigraphy analysis and diagenesis evolution of a Barremian carbonate platform (Kharaib Formation), Onshore Abu Dhabi, United Arab Emirates. *In*: Abu Dhabi International Petroleum Exhibition & Conference. *Annals…* SPE-188875-MS. https://doi.org/10.2118/188875-MS

Tuttle M.L.W., Charpentier R.R., Brownfield M.E. 1999. The Niger Delta petroleum system: Niger delta province, Nigeria, Cameroon, and Equatorials Guinea, Africa. *United States Geological Survey Open-File Report*, 99-50-H, 65 p.

Van Wagoner J.C., Mitchum Jr. R.M., Campion K.M., Rahmanian V.D. 1990. Siliciclastic sequence stratigraphy in well logs, core, and outcrops: concepts for high-resolution correlation of time and facies. *American Association of Petroleum Geologists Methods in Exploration Series*, **7**, 55 p.

Van Wagoner J.C., Posamentier H.W., Mitchum R.M. Jr., Vail P.R., Sarg J.F., Loutit T.S., Hardenbol J. 1988. An overview of sequence stratigraphy and key definitions. *In*: Wilgus C.K., Hastings B.S., Kendall C.G.St.C., Posamentier H.W., Ross C.A., Van Wagoner J.C. (eds.). *Sea level changes:* an integrated approach. Society of Economic Paleontologists and Mineralogists Special Publication, **42**:39-45.

Wilgus C.K., Hastings B.S., Kendall C.G.St.C., Posamentier H.W., Ross C.A., Van Wagoner J.C. (eds.). 1988. *Sea level changes:* an integrated approach. Society of Economic Paleontologists and Mineralogists Special Publication, **42**, 407 p.

Wright V.P., Marriott S.B. 1993. The sequence stratigraphy of fluvial depositional systems: the role of floodplain sediment storage. *Sedimentary Geology*, **86**(3-4):203-210. https://doi.org/10.1016/0037-0738(93)90022-W

Zampetti V., Perrotta S., Chaari G., Krayenbuehl T., Braun M., Neves F., Hu J. 2017. Seismic Characterization of the Shuaiba Formation in the Western Region of UAE, a Predictive Tool to unravel Shuaiba Facies Mosaic? *In*: Abu Dhabi International Petroleum Exhibition & Conference, 2017, Abu Dhabi. *Annals…*, SPE-188346-MS, p. 1-12. https://doi.org/10.2118/188346-MS

Zhukov V.V., Bogatyrev B.A. 2012. Dynamic models of lateritic bauxite formation. *Geology Ore Deposits*, **54**:370-397. https://doi.org/10.1134/S1075701512050066